MICROSTRUCTURES AND TRACE ELEMENT SIGNATURES
OF OROGENIC QUARTZ VEINS IN THE KLONDIKE DISTRICT,
YUKON TERRITORY, CANADA

by

W.R. GARETH WOLFF

A THESIS SUBMITTED IN PARTIAL FULFILLMENT OF
THE REQUIREMENTS FOR THE DEGREE OF

BACHELOR OF SCIENCE (HONOURS)

in

THE FACULTY OF SCIENCE
(Geological Sciences)

This thesis conforms to the required standard

....
Supervisor

THE UNIVERSITY OF BRITISH COLUMBIA
(Vancouver)
APRIL 2012

ABSTRACT

The rich placer gold deposits of the Klondike District in the Yukon Territory are derived from orogenic gold-bearing quartz veins, associated with the metamorphism of the Klondike Schist basement rock. Further understanding of the structural context of these veins may be essential for exploration in the region. Petrographic descriptions were made of 12 polished thin sections of Klondike vein samples, observing vein and host rock mineralogy and microtextures. Two broad textural categories were identified: blocky veins produced by a single fracturing event with dilation rate exceeding the rate of quartz growth into open space; and elongate-blocky to fibrous veins with the average rate of opening equal to the average rate of quartz growth. The structural interpretation of this variation is of an early stage of slow vein growth, producing fibrous quartz grains, as well as gold and sulphides. Later rapid fracturing led to the growth of blocky quartz. This variation in vein textures can be attributed to structural changes, and the progression through the brittle-ductile transition in the crust. Polished blocks of texturally complex samples from the Nugget and Sheba veins were analyzed by laser ablation ICP-MS, producing trace element concentrations for the different quartz textures. Aluminium was the most abundant trace element, and orogenic quartz was found to have low concentrations and variability of trace elements when compared with higher temperature magmatic-hydrothermal systems. No significant compositional variations were found, indicating that despite the broad textural differences, there were no significant changes in the physical and chemical conditions of quartz growth, or in the fluid in equilibrium with the host rock.

TABLE OF CONTENTS

LIST OF FIGURES

LIST OF TABLES

ACKNOWLEDGEMENTS

1.0 INTRODUCTION

The Klondike District of the Yukon Territory is renowned as one of the world's richest regions of placer gold deposits, with estimates of total historical production surpassing 13 million ounces of placer gold since its initial discovery in 1896 (Chapman et al., 2010a). The placer deposits have been associated with orogenic gold-bearing quartz veins hosted in the greenschist facies Klondike Schist basement (MacKenzie et al., 2008).

The richness of the placer gold deposits, as well as the relatively small volume of eroded basement rock (possibly as little as 400km^2 of basement (MacKenzie et al., 2008)), suggest very high concentrations of orogenic lode gold in the area. However, until recently very limited research had been published on the geology and structure of the gold-bearing veins.

The Yukon Gold Project is a large, industry-supported multidisciplinary research project by the Mineral Deposit Research Unit at the University of British Columbia, that among its goals attempts to address the geologic context for gold exploration in the region. This includes detailed structural and geochemical analysis of the gold-forming veins in the Klondike.

As a part of the broader study, this thesis aims to use quartz vein microtextures and trace elements to help unravel the structural history of gold-forming veins in the district. Petrographic observations are coupled with laser ablation ICP-MS trace element measurements for a set of samples from cm-scale quartz veins. This will contribute to the body of knowledge on orogenic quartz, as well as potentially determine the controlling factors on the different textures observed in the region, and any textural controls on trace element concentrations.

2.0 BACKGROUND & PREVIOUS WORK

2.1 Klondike District: An Overview

2.1.1 Geological Setting

The Klondike District is a region of the Yukon Territory, near the northeast boundary of the Yukon-Tanana Terrane, about 400km northwest of the city of Whitehorse. The bedrock

geology of the district, along with the gold-bearing vein systems it contains, have been discussed and described by Mortensen (1990), Knight et al. (1999), MacKenzie et al. (2008) and Chapman et al. (2010a, b).

The basement that underlies the Klondike District is predominantly composed of three variably metamorphosed rock units, forming an imbricated structural stack (Chapman et al, 2010a), locally separated by lenses of ultramafic rocks (Mortensen, 1990, 1996, MacKenzie et al., 2008). The structurally uppermost units, in which all the known orogenic gold occurrences are hosted, form part of the Klondike Schist. This Late Permian assemblage consists mainly of middle greenschist facies mafic and felsic metavolcanic rocks (chlorite-actinolite schist and pyritic quartz-muscovite schist), and their intrusive equivalents (quartz-feldspar augen schist, quartz monzonite gneiss, and metagabbro), as well as interlayered siliciclastic rocks and rare carbonaceous schist (Chapman et al., 2010a).

These uppermost thrust slices of the Klondike Schist are structurally stacked on top of the Late Devonian-Early Mississippian Nasina assemblage, a package of carbonaceous metaclastics with minor marble. Additionally, metamorphosed greenstones of the Slide Mountain Terrane are present as lenticular bodes along several of the main thrust fault contacts separating individual units of the Klondike and Nasina schists (MacKenzie et al., 2008, Chapman et al., 2010a). These generalized bedrock associations can be observed in Fig. 1.
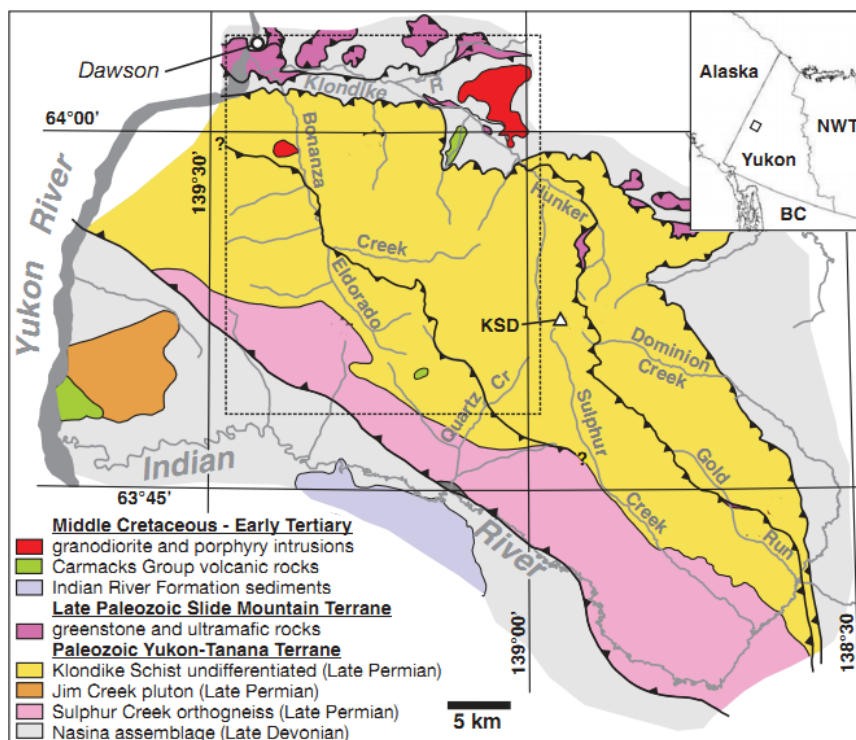
Figure 1: *Simplified bedrock geology map of the Klondike District. KSD = King Solomon Dome. (Modified from Chapman et al., 2010a)*

Uplift in the area was likely initiated in the late Jurassic and continued into the mid-Cretaceous, with deposition of basin-filling conglomerates of the Indian River Formation. Regional extension and normal faulting in the Late Cretaceous affected the Klondike Schist and surrounding region, and was accompanied by the eruption and deposition of Carmacks Group volcanic rocks (MacKenzie et al., 2008). In the Paleocene, the initiation and consequent strike-slip motion of the Tintina Fault caused additional regional extension (Gabrielse et al., 2006, MacKenzie et al., 2008). The Tintina Fault, a major right-lateral strike-slip fault with approximately 400-450km of displacement (Lowey, 2006), offset the Finlayson Lake assemblage in the southeast Yukon from the Klondike District and the rest of the Yukon-Tanana Terrane (Lowey, 2006, Gabrielse et al., 2006, MacKenzie et al., 2008).

Erosion of the Klondike Schist during Late Tertiary regional uplift resulted in the deposition of the Pliocene age White Channel Gravels, in flat-bottomed valleys formed by braided streams (MacKenzie et al., 2008, Chapman et al., 2010a). Erosional downcutting of this older drainage system occurred in the Pleistocene to Holocene, with modern streambeds lying up to 70m below the White Channel depositional surface (Chapman et al., 2010a).

Placer gold deposits in the area are associated with both the White Channel Gravel unit and the low-level gravels produced by the younger streams. The gold in the low-level gravels has been either eroded and reworked from the White Channel Gravel, or eroded directly from bedrock in the area (Lowey 2006, Chapman et al., 2010a). The Klondike District was not affected by Pleistocene glaciation, allowing the placer deposits to be connected directly to the local uplift and erosion (Chapman et al., 2010a).

2.1.2 Structural Processes

MacKenzie et al. (2008) undertook a structural study of the Klondike Schist, in order to identify structural controls on the formation of the orogenic veins. They established five different deformation events recorded in the rocks of the Klondike District (MacKenzie et al., 2008, Chapman et al., 2010a).

The first of these stages (D_1) involves the development of a pervasive metamorphic foliation (S_1), that is sheared into parallelism with a second pervasive fabric (S_2). Metamorphic segregation quartz veins also developed parallel to S_2, on the mm- to cm-scale. The Nasina Schist has similar pervasive foliation, albeit finer-grained, whereas the Slide Mountain Terrane greenstones are mostly unfoliated and contain no biotite. The entire stack

has been metamorphosed to greenschist facies, dominated by quartz, muscovite, chlorite and sporadic biotite in the Klondike and Nasina Schists, and albite, chlorite and epidote in the greenstones (MacKenzie et al., 2008).

The third stage consists of thrust emplacement (D_3), resulting in post-metamorphic folds (F_3) with rounded hinges. A variably developed spaced cleavage (S_3), parallel to the axial surfaces of the folds, dominates the rock fabric around hinge zones of recumbent folds in the Nasina and Klondike Schists. In the greenstones, S_3 is limited to narrow zones near thrust zones. Chlorite and muscovite recrystallization is present along the spaced cleavage in the Klondike Schist folds, and chlorite is also present in the greenstones. However, in the Nasina Schists there is little mica recrystallization. An additional stage of D_3 involves the reactivation of the S_2 foliation and/or S_3 spaced cleavage on some surfaces, producing a shear cleavage—this is not present in the greenstones. (MacKenzie et al., 2008)

The D_4 stage is comprised by two sets of localized, steeply-dipping reverse faults and associated kink folds (F_4), mainly striking north-west. The Nasina Schist contains only minor kink folding, and this stage is absent from the greenstones (MacKenzie et al., 2008, Chapman et al., 2010a). Orogenic veins in the Klondike (see below) occupy S_4 deformation zones (MacKenzie et al., 2008).

Finally, Late Cretaceous normal faulting (D_5) occurred during regional extension (Mortensen, 1996, MacKenzie et al., 2008). The faults were mostly localized by pre-existing structural weaknesses, which in the Klondike tend to stem from the D_4 stage. The fault zones contain abundant gouge development, and are usually hydrothermally altered, pyritized, and silicified (MacKenzie et al., 2008).

2.1.3 Klondike Quartz Veins

Orogenic quartz veins are extensional veins associated with deformed and metamorphosed terranes, and are examined in more detail below. Two types of orogenic quartz veins are present throughout the Klondike. Segregation veins, lens-shaped, parallel to foliation, and mineralogically similar to the host rocks, are widespread throughout the district and found in all metamorphic lithologies (Rushton et al., 1993, Chapman et al., 2010a). MacKenzie et al. (2008) attributes this first generation of veining as the first two phases of ductile deformation (D_1-D_2). These veins do not contain gold or sulphides, except where cut by later fractures (Rushton et al., 1993, Chapman et al., 2010a).

Meanwhile, massive, milky quartz veins, up to 3m thick and up to hundreds of metres in strike length, are generally discordant to the metamorphic foliation (Rushton et al., 1993). These veins are gold-bearing, and occur both as scattered individual veins and swarms. They generally trend north-northwest, and are apparently controlled by the F_4 fold axial surface fractures. The density of veining is highest in zones of locally high strain, related to fault-fold deformation zones. MacKenzie et al. (2008) interpret this vein generation to have formed following (or late in) the D_4 deformation event, predating (and locally cross-cut by) the Late Cretaceous normal faulting. The veins are composed predominantly of quartz, with minor Fe-carbonate, barite, scheelite, sulphides and sulphosalts, and gold (Chapman et al., 2010a).

The gold is commonly associated with pyrite, typically in selvages along the margins of veins. Occasional free grains of gold within the vein quartz are also present. The deposition of the gold is suggested as resulting in part from sulphidation of the wall rocks and resultant destabilization of bisulphide complexes in the mineralizing fluids (Rushton et al., 1993, Chapman et al., 2010a). Vein formation appears to be from a single-stage process rather than repeated fluid pulses (Chapman et al., 2010a), although recent field studies have shown vein formation to be much more episodic than previously suggested (M. Allan, personal communication, 2011).

Using trace element concentrations of gold particles from both the lode gold vein deposits and the extensive placer gold in the district, Knight et al. (1999) concluded that the placer deposits were predominantly—if not entirely—derived from the orogenic vein deposits. Lowey (2006) agreed with this conclusion.

2.2 Orogenic Gold Deposits

Orogenic vein gold deposits, also occasionally termed mesothermal, are epigenetic deposits hosted in deformed and metamorphosed rocks. They are typically composed of gold-bearing quartz (and carbonate) fault-fill veins in moderately to steeply dipping, compressional ductile-brittle shear zones and faults (Dubé and Gosselin, 2007). In Pre-Cambrian examples, mafic rocks metamorphosed to greenschist (and locally lower amphibolites) facies at intermediate depths (5-10km) provide the dominant host (Dubé and Gosselin, 2007), although Phanerozoic examples are largely hosted by greenschist metasediments. Fig. 2 illustrates a simplified model for these deposit types. A detailed classification study by Groves et. al (1998) allows the placement of these deposits in context with other gold deposit types, although the topic remains controversial.
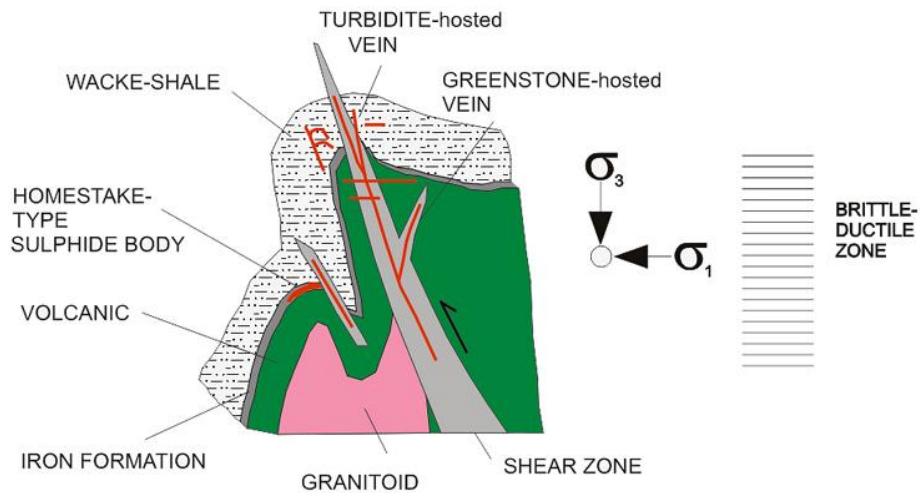
Figure 2: Schematic diagram of orogenic quartz vein deposit setting. (From Dubé and Gosselin, 2007)

A leading model for orogenic gold formation describes veins forming along convergent margins during terrane accretion, translation or collision, in deformed accretionary belts alongside continental magmatic arcs. They are emplaced during compressional to transpressional regimes (Groves et al., 1998, 2003). There is strong structural control on the deposits, generally involving major crustal faults, shear zones, folds, or zones of competency contrasts (Groves et al., 1998, 2003, Dubé and Gosselin, 2007).

The fluids responsible for the formation of the ore have been determined to be low-salinity, dilute, mixed aqueous-carbonic fluids; using isotope studies (Jia et al., 2003) and fluid inclusion studies (Ridley and Diamond, 2000, Groves et al., 2003). Dubé and Gosselin (2007) summarize the ore depositional process as a metamorphic Au-transporting fluid structurally channelled to shallow crustal depths. The gold is transported as a reduced sulphur complex (Groves et al., 2003). Due to fluid-pressure cycling processes, as well as geochemical gradients in temperature, fS_2, fO_2, and pH, the fluid is then precipitated as vein material or wall-rock replacement, in second and third order structures at shallow crustal levels (Dubé and Gosselin, 2007).

One of the major outstanding problems with the model of orogenic vein gold deposits lies in the source of the fluids. Most workers favour a deep origin, with the input of meteoric waters considered unlikely (Goldfarb et al., 2005, Dubé and Gosselin, 2007). However, options such as deeper levels of the ore-hosting volcano-sedimentary or sedimentary terranes,

6

or deeper metamorphic sources such as subducted oceanic crust, are debated (Groves et al., 2003). The lithological source of the gold is also disputed, in particular whether a crustal pre-concentration is required (Groves et al., 2003).

Other areas where knowledge gaps remain include the configuration of fluid-flow paths in the system, and the fluid flow itself; the timing of mineralization; and the depositional mechanism (Groves et al., 2003, Dubé and Gosselin, 2007).

2.3 Trace Elements in Quartz

Quartz (chemical formula SiO_2) is one of the most abundant minerals in the Earth's crust, and the most important silica mineral (Götze 2009). It is found in veins in a variety of hydrothermal and magmatic systems, precipitating from hydrothermal fluids of a variety of compositions at temperatures from 50-750°C (Rusk et al., 2008). Quartz may contain varying concentrations of trace elements, with titanium and aluminium among the most common, either through incorporation into the crystal structure or bound as microinclusions (Götze et al., 2004).

Trace elements in quartz are in part a product of the chemistry of the fluid of origin, and therefore may prove representative of the environment of crystallization for the quartz (Landtwing and Pettke, 2005, Donovan et al., 2011). As a consequence, trace element concentrations in quartz have become a focus of study in recent years. For example, Götze et al. (2004) examined trace elements in pegmatitic quartz, as did Beurlen et al. (2011).

Landtwing and Pettke (2005) combined scanning electron microscope cathodoluminescence microscopy (SEM-CL) studies with laser-ablation inductively coupled-plasma mass-spectrometry (LA-ICP-MS) trace element studies of a porphyry Cu-Au-Mo deposit in Utah, and concluded that more trace elements are incorporated into quartz at higher growth rates, which they concluded as corresponding to greater degrees of disequilibrium. A similar study by Rusk et al. (2006) at a porphyry copper deposit in Montana, also using SEM-CL and LA-ICP-MS, determined that different generations of quartz can be distinguished based on unique trace element contents. This study also correlated titanium with temperature of quartz precipitation.

Similar correlations for Ti concentrations and crystallization temperature of quartz were found in topaz-bearing granites in the Czech Republic by Müller et al. (2003), where an electron probe micro-analysis (EPMA) study associated high Ti (>40ppm) with high crystallization temperature and pressure of quartz phenocrysts. Allan and Yardley (2007) also

found high Ti correlating with high temperatures, in an SEM-CL, secondary isotope mass spectrometry (SIMS), and LA-ICP-MS study observing CL, oxygen isotopes and trace elements for a magmatic-hydrothermal system in Australia. They also interpreted variations in Al and Li as corresponding to shifts in quartz precipitation rate.

The relationship between Ti substitution for Si in quartz and the temperature of equilibration was investigated in further depth by Wark and Watson (2006), who equilibrated quartz with rutile (TiO_2) in the presence of aqueous fluids and/or silicate melt at temperatures from 600 to 1,000^{o}C, and experimentally developed a titanium-in-quartz geothermometer (referred to as the TitaniQ). Rusk et al. (2008) applied this geothermometer to hydrothermal ore deposits formed between ~100 and ~750°C, and in addition to reaching the same conclusion on Ti, concluded from bimodal Al concentrations in lower temperature samples that Al concentrations in quartz reflect fluctuations in pH. A further study (Rusk et al., 2011), using LA-ICP-MS to examine four different ore deposit types (Carlin-type Au, epithermal Au, porphyry-Cu and MVT Pb-Zn), also found variations in Al concentrations of up to two orders of magnitude for samples at temperatures <300°C, and correlations Li, Na, and K with Al.

2.4 Vein Microstructures and Growth

Veins are formed by the combination of brittle failure and void formation, followed by fluid flow and precipitation through the resulting conduits (Hilgers and Sindern, 2005). These processes can happen multiple times, with the result that individual veins can record several crack-seal events (Ramsay, 1980, Hilgers and Sindern, 2005).

During these deformation events, different vein microstructures can develop. Elongate crystals are among the most useful of these structures, due to the kinematic information they provide on progressive deformation in rocks (Hilgers et al., 2001, Hilgers and Sindern, 2005). For the purposes of this thesis, veins are subdivided into three broad textural categories, based on the scheme of Oliver and Bons (2001): (1) fibrous veins (with length to width ratios of 10 to >100); (2) elongate-blocky veins; and (3) stretched crystal veins.

Hilgers and Sindern (2005) and Hilgers and Urai (2002) summarize the different growth mechanisms of syntectonic elongate vein microstructures (Fig. 3.), classifying them as *antitaxial*, *syntaxial*, and *stretched* or *ataxial*. Antitaxial veins consist of fibrous veins growing towards the vein-wall interface. The growth direction is indicated by an increase in the width of the fibres towards the contact between the vein and the wall. Small crystals are

positioned along the centre of the vein, forming a 'median line'. (Hilgers and Sindern, 2005). The vein material precipitates at the vein-wall boundary, with a compositional discontinuity thus existing between vein and host rock (Hilgers and Urai, 2002). For such fibrous grains to form, the growth competition between adjacent grains must be limited by a narrow aperture (Oliver and Bons, 2001).
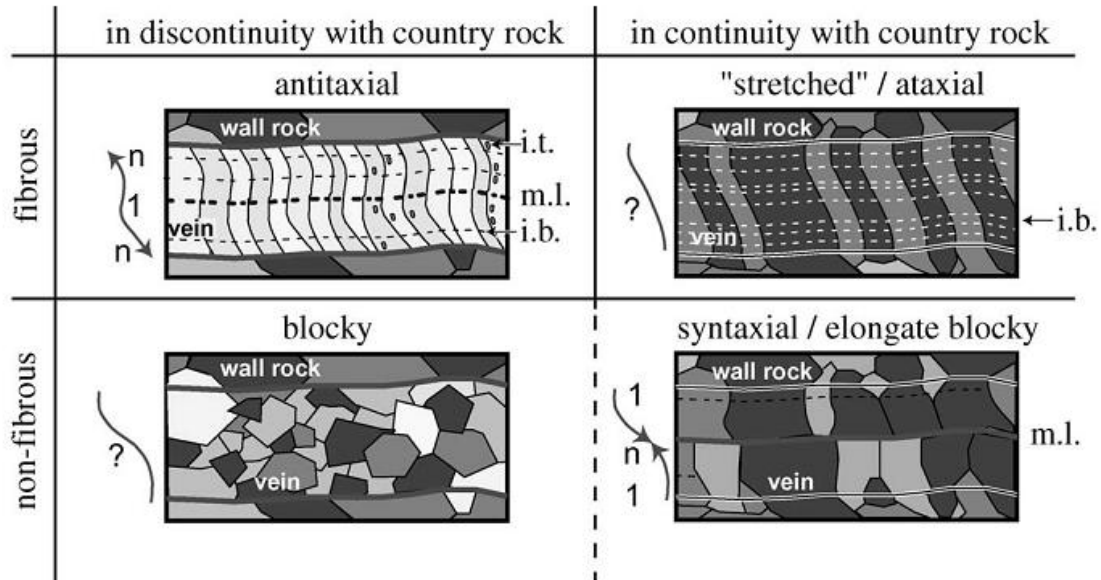
Figure 3: *Classification of veins according to grain morphology and crystal growth. Arrows indicate opening direction. m.l.= median line, i.b. = inclusion bands, i.t. = inclusion trails. (From Hilgers and Urai, 2002)*

In syntaxial veins, the grains are elongate-blocky rather than fibrous, and grow from the wall into the vein, as epitaxial overgrowths of the wall rock (Hilgers and Sindern, 2005). These veins show clear signs of growth competition (Oliver and Bons, 2001).

Ataxial veins, or stretched crystals, consist of columnar fibres with jagged grain boundaries that cross the vein from one wall to the other, connecting grains in the wall rock. They are of the same composition as the material in the wall rock, and are believed to have been formed by repeated fracturing and growth at alternating sites in the vein (Hilgers and Sindern, 2005). Ataxial veins usually contain solid and fluid inclusions arranged parallel to the vein-wall boundary (Hilgers and Urai, 2002).

Hilgers and Urai (2002) also mention entirely non-fibrous *blocky* veins, where the direction of growth is unclear. These are the result of ongoing crystal nucleation after vein formation, which is primarily caused by high supersaturation of vein-forming minerals (Oliver and Bons, 2001).

For the growth of syntectonic veins, crystal morphology is dominantly controlled by the relative rates of crystal growth velocity and dilation, and the width of the opening increment

(Hilgers and Urai, 2002). Thus, if the vein opens at the same rate as crystal growth, elongate and fibrous textures are formed, whereas if the opening rate is greater than the crystal growth, the crystals grow into a free space and produce blocky or euhedral textures (Hilgers et al., 2001).

3.0 RESEARCH QUESTION

The gold-bearing orogenic quartz veins of the Klondike District contain a variety of microtextures and microstructures, with variation both between veins and across the width of single veins. Different textures of quartz, from the margin to the centre of the vein, may indicate varying growth rates and environments, and may represent discrete stages of fluid flow. Thus, it is possible to infer an evolution in physical and chemical conditions during the lifetime of the vein.

One possible way of tracking this geochemical evolution is an examination of trace element compositions. As reviewed in the previous section, there are several existing studies attempting to use quartz trace element chemistry as an indicator of fluid geochemistry. The goal of this investigation is to refine these existing studies to focus on the trace element concentrations of orogenic quartz veins, an area of study that is currently lacking in detailed research.

Therefore, the question that this thesis seeks to address is: can trace element concentrations of orogenic quartz be used to help interpret the conditions of formation of these veins, and more importantly, whether these conditions changed during vein formation? The study intends to test the hypothesis that different quartz textures are a product of changing physical and chemical conditions of formation, and that these changes will be reflected in the trace element concentrations. Important variables include the geochemistry and pressure-temperature conditions of the originating fluid. The study combines petrographic examinations of hand samples and polished sections with trace element measurements using laser ablation ICP-MS analysis, for a set of gold-bearing quartz veins in the Klondike District of the Yukon Territory in northwestern Canada (Fig.4).

There is at present little research on the trace element chemistry of lower temperature orogenic quartz veins that have no apparent magmatic input. In particular, the use of Ti in quartz as a geothermometer (Wark and Watson, 2006), a study which did not go below

600°C, may nevertheless serve as a qualitative proxy for temperature in lower temperature systems.
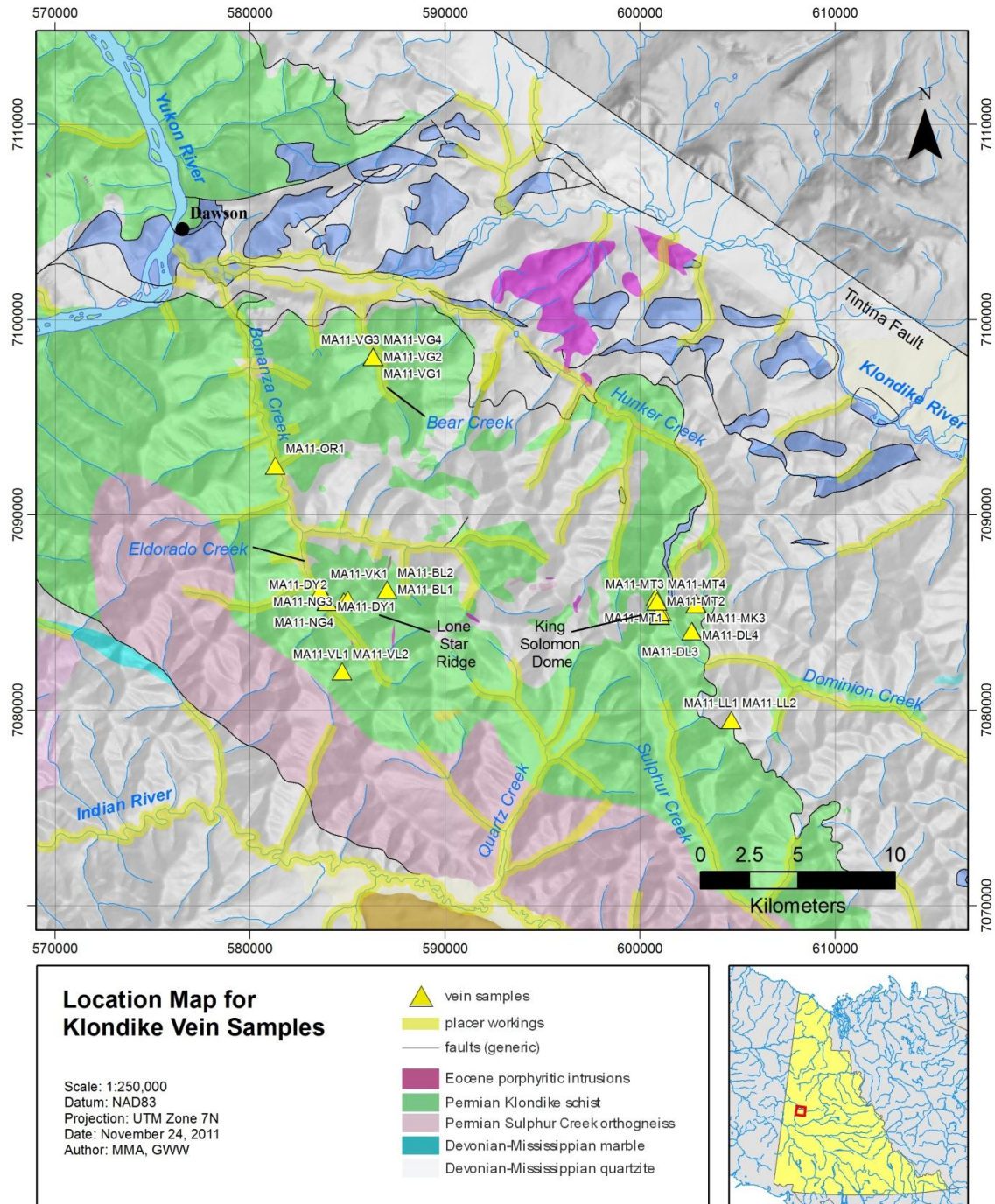
Figure 4: Location Map for studied vein samples.

This study aims to use spatial variations in trace element chemistry as a potential means of explaining the textural variations. By examining cm-scale quartz veins, it is possible to study a cross-section across the entire vein. Such a cross-section may then be scaled up to produce

a picture of variations across much larger-scale orogenic veins—although one must be conscious that larger veins may record many more events than the narrower veins.

This pilot study may contribute valuable insight into the fluid geochemistry and formation processes of orogenic veins. The discordant orogenic veins in the Klondike are considered the major origin of the placer gold deposits in the district, as well as containing substantial lode gold resources (Knight et al., 1999). However, the exact mechanisms of vein formation are still poorly constrained. A better understanding of the veins—and consequently, the gold deposits—would be invaluable for future exploration of the region. Additionally, the study contributes to a growing body of literature on how quartz composition varies across different geologic environments.

4.0 METHODS

4.1 Sample Preparation

A set of 14 samples of orogenic quartz veins from the Klondike were selected (Table 1). These samples were collected by Dr Murray Allan during the summer of 2011. Relatively narrow veins were selected to permit microtextural and microchemical analysis across the entire width of the vein, where possible.

Table 1: *List of Samples Analyzed*

VEIN	SAMPLE NUMBER	NOTES
Aime	MA-11-AM2	
	MA-11-AM3	
Dysle	MA-11-DY1	
	MA-11-DY2	
Lloyd	MA-11-LL2	No thin section
Mackay	MA-11-MK2	
Nugget	MA-11-NG2	
	MA-11-NG4	Trace element analysis
	MA-11-NG5	
Orofino	MA-11-OR1	
Sheba	MA-11-SH	No thin section
	MA-11-SH3	Trace element analysis
Virgin	MA-11-VG2	
Violet	MA-11-VL2	

Rectangular billets were cut from the rocks, with two approximately parallel off-cuts from each rock, with approximate rectangular dimensions of 4 x 2cm, and thickness between 0.2 and 1cm. One of each pair of billets were prepared as polished thin sections at the University of Utah College of Mines and Earth Sciences. The remaining off-cuts were ground and polished by hand to a 3 micron polish, for laser ablation.

4.2 Laser Ablation ICP-MS

Trace elements in the quartz from the polished blocks and thin sections were analyzed using a Resonetics RESOlution M-50-LR laser ablation unit connected to an Agilent 7700 series ICP-MS (at the Pacific Centre for Isotopic and Geochemical Research at the University of British Columbia), with the assistance and supervision of Dr Shaun Barker. A preliminary set of line rasters were run on the blocks. Due to quartz spallation and concerns over surface contamination, the raster method was then replaced by spot traverses.

For samples MA-11-NG4 and MA-11-SH3, both thin sections and blocks were ablated at 5Hz and 80mJ over 64μm spots. The spots were correlated with scanned images of the blocks and photomicrographs of the thin sections (Appendix II). Glass standard SRM 612 from the National Institute of Standards and Technology (NIST) was used as an external calibration standard, with Columbia River Basalt (BCR) from the U.S. Geological Survey used as an additional standard. Isotopes analyzed were ^{7}Li, ^{23}Na, ^{27}Al, ^{29}Si, ^{39}K, ^{43}Ca, ^{47}Ti, ^{57}Fe, ^{69}Ga, ^{72}Ge, ^{75}As, ^{88}Sr, ^{118}Sn, ^{121}Sb, and ^{137}Ba. The internal standard element was Si in quartz, set to a default concentration of 46.74 wt.%.

4.3 Data Reduction and Analysis

The raw trace element data was integrated using Iolite software from the University of Melbourne (Figs. 5 and 6). For each spot, a window of data was selected, attempting to avoid surface contamination and spikes due to inclusions or spallation during ablation. Additionally, for the thin sections, the selected data window avoided the glass slide (Fig. 6).

The reduced data was then exported to a spreadsheet, and trace elements were plotted for each section, distinguishing between the different quartz textures within each sample.

13
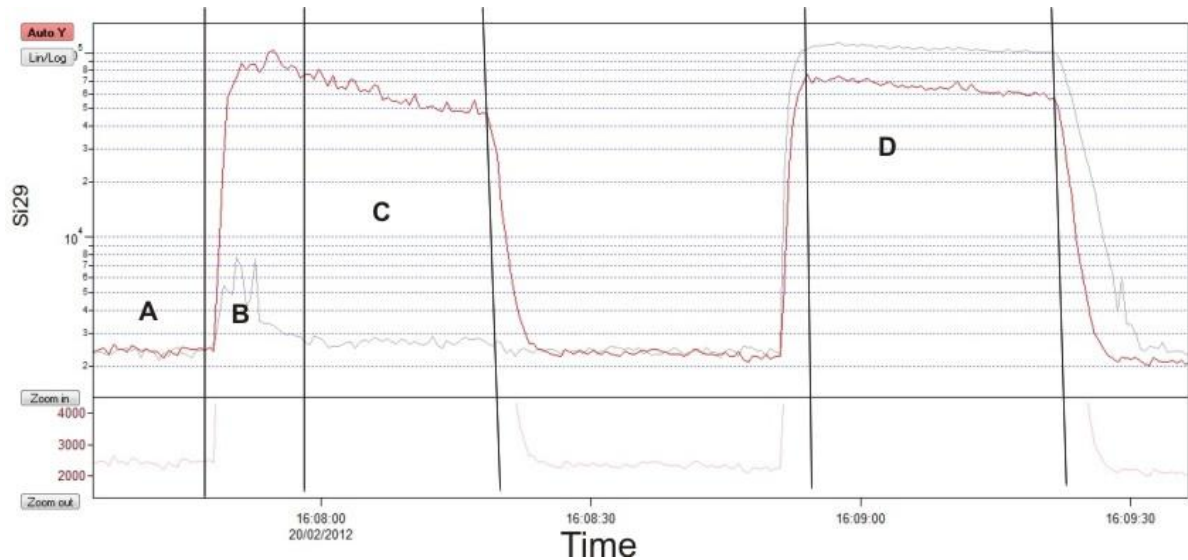
Figure 5*: Raw trace element data for sample 'NG4_thick'. Red trace = Si29, grey trace = Na23. A = background signal; B = surface Na spike, likely surface contamination; C = integrated window for vein quartz spot; D = integrated window for NIST 612 spot.*
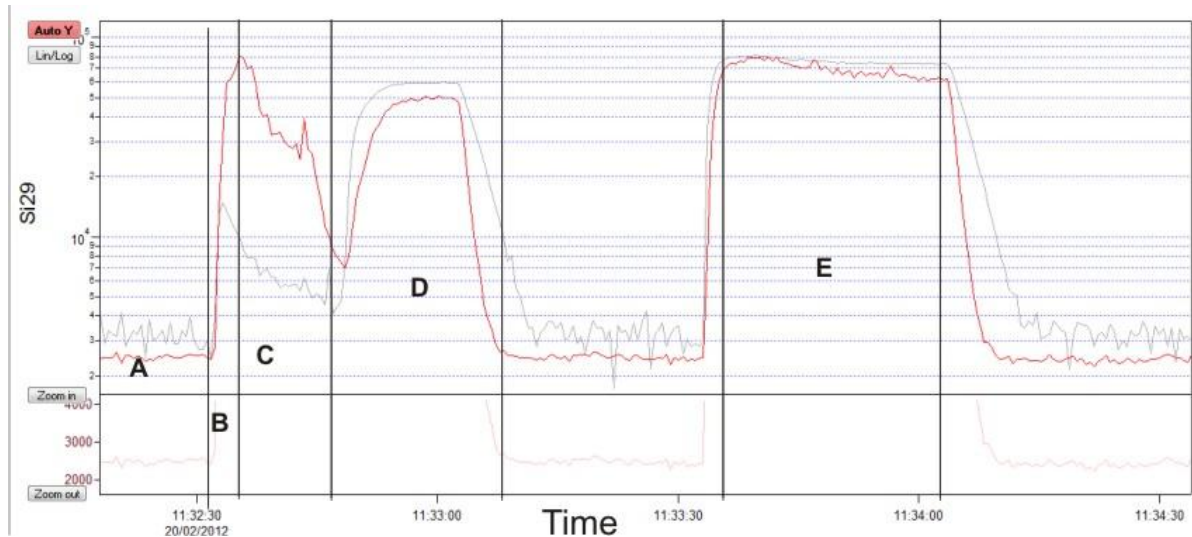
Figure 6*: Raw trace element data for sample 'SH3_thin'. Red trace = Si29, grey trace = Al27. A = background signal; B = surface of thin section; C = integrated window for vein quartz spot; D = signal from glass slide; E = integrated window for NIST 612 standard spot.*

4.4 Petrography

Using both reflected and transmitted light microscopy, petrographic descriptions were made of the thin sections. The mineralogy of both vein and wall rock was examined, as were the different microstructures within the veins and their associations at the vein-wall rock interface. Contextual descriptions were also made of the original hand samples from which the billets were cut.

14

5.0 VEIN MICROSTRUCTURES

5.1 Textural Observations

Among the 12 polished thin sections that were examined by reflected and transmitted light microscopy, a limited number of textures were observed. Detailed descriptions of the thin sections can be found in Appendix I.

The host rock is muscovite-chlorite-quartz-feldspar schist, with muscovite and chlorite comprising ~20-70%, and a fine-grained, granoblastic, quartzofeldspathic groundmass comprising the remainder. An exception is sample MA-11-NG2, in which medium-grained laths of plagioclase feldspar make up ~75% of the host rock.

Blocky, subhedral to anhedral intergrown quartz dominates the veins, with varying degrees of deformation. The vein-wallrock boundary is generally characterized by a band of much finer grained quartz. Fine-grained, recrystallized quartz is common along fracture planes and grain boundaries, and most veins contain wallrock inclusions in the form of interstitial and included fine-grained micas, many of which preserve host rock mineralogy and textures. Iron carbonate alteration is present in many samples.

Other quartz textures include elongate-blocky quartz (e.g., Nugget vein samples MA-11-NG2 and MA-11-NG4) and fibrous quartz (e.g., MA-11-NG4 and MA-11-SH3). The Nugget vein has the greatest observed variation in vein textures. Euhedral to subhedral calcite is also present in the Nugget vein samples.

Highly oxidized, subhedral to euhedral sulphides are found in several of the vein samples. Pyrite makes up the bulk of the sulphide content, with arsenopyrite also present (in sample MA-11-SH3). Where present, the sulphides appear either in isolated grains or as a cluster of fine grains, and make up ~1% or less of the overall assemblage. They can be observed in both the host rock (primarily) and the veins, but in all cases are spatially associated with the vein wall and, where present, the fibrous quartz textures.

Based on the spatial associations of the different quartz textures and the sulphides, a paragenetic model for the Klondike orogenic veins can be summarized as an early stage of fibrous and elongate-blocky quartz growth, associated with sulphides and gold, and a later stage of blocky, barren quartz growth (Table 2). Later hydrothermal processes led to widespread recrystallization of quartz and the growth of euhedral to subhedral quartz and calcite into pre-existing voids.

Table 2: *Generalized paragenesis of Klondike veins.*

	Early		Late
Fibrous + elongate-blocky quartz	▬▬▬▬		
Arsenopyrite + pyrite	▬▬▬		
Gold	▬▬▬		
Fe-carbonate	▬▬▬ ···········		
Blocky quartz		▬▬▬	
Subhedral + recrystallized quartz			▬▬▬
Subhedral to euhedral calcite			▬▬▬

5.1.1 Nugget Vein

Three different samples from the Nugget vein were studied, and a variety of textures were observed. In sample MA-11-NG2, highly deformed, finely fractured elongate-blocky quartz grains grow across the vein, intergrowing with euhedral to subhedral plagioclase laths at the vein boundary.

Sample MA-11-NG5 includes the intersection of two minor veins (Fig. 7) with one cutting almost perpendicularly across the pre-existing vein. The area of intersection contains strongly deformed quartz with abundant inclusions and fine recrystallized interstitial grains. However, both veins are texturally very similar, consisting of anhedral to subhedral blocky quartz.
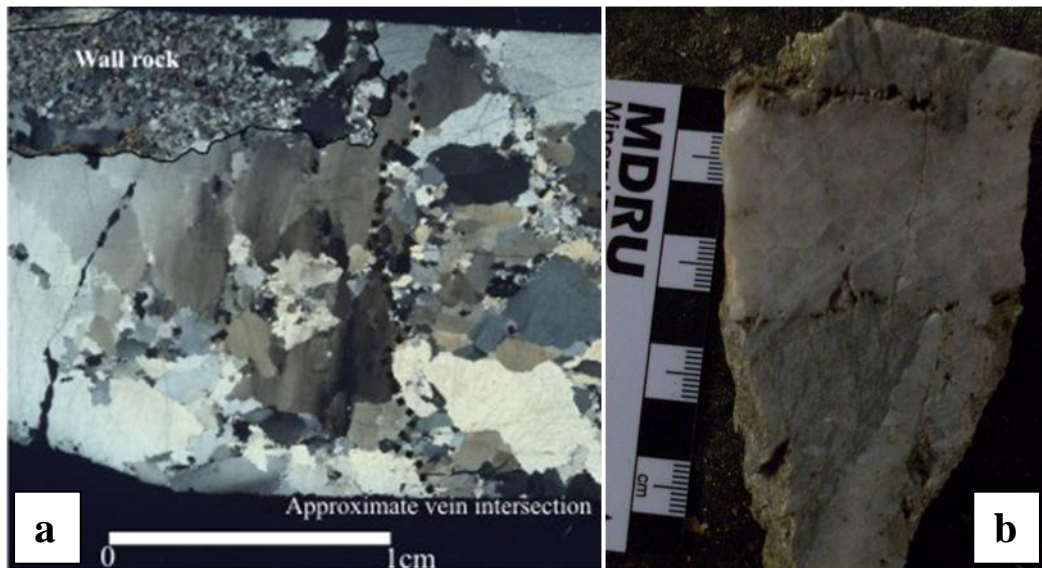
*Figure 7: Sample MA-11-NG5. **a.** Photomicrograph of sample, XPL. Dotted line = approximate intersection between different stages of quartz veining. **b.** Photograph of vein intersection in hand sample, cut surface.*

Sample MA-11-NG4 (Fig. 8) is texturally complex, containing two stages of fibrous quartz, elongate-blocky quartz, simple blocky quartz, and late subhedral quartz and calcite. As the fibrous quartz extends away from the wallrock, there is evidence of growth competition as grains widen into elongate-blocky crystals (with a length to width ratio of less than 10). This is particularly apparent in the bottom half of the section. Meanwhile, in the top half, at the line labelled 'E' on Fig. 8 there is a boundary between elongate quartz fibres and blocky quartz. To add to the complexity of the sample, there is an isolated region of fibrous quartz ('G' on Fig. 8), surrounded on all sides by the blocky grains.

In addition, subhedral, blocky quartz grains are scattered throughout the section, particularly clustered along the edge of the largest elongate-blocky crystal, and associated with prismatic calcite ('H' on Fig. 8; the calcite is identifiable by its third-order interference colours). These indicate growth into free void space.
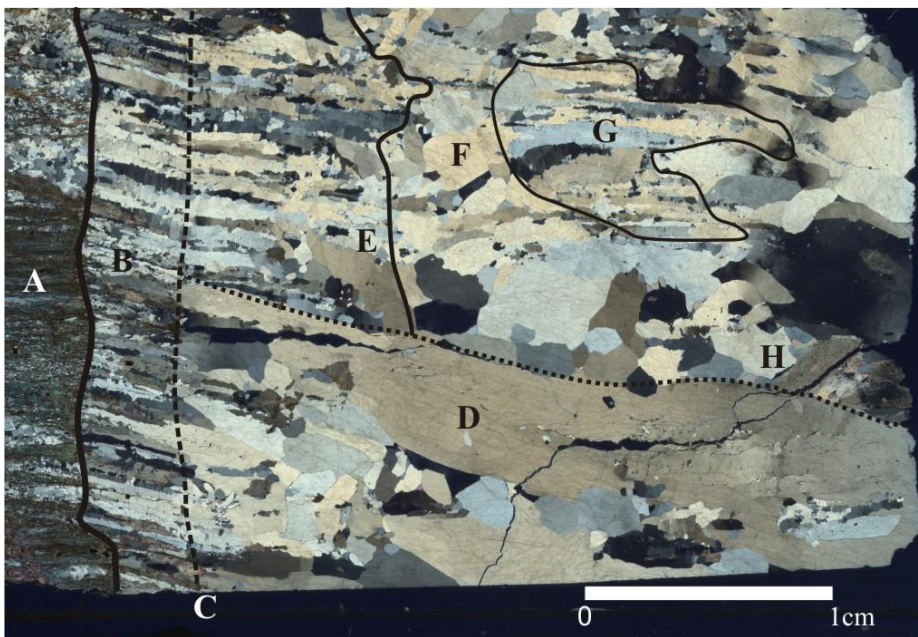
Figure 8: *XPL photomicrograph of sample MA-11-NG4. A = wallrock; B = syntaxial fibrous quartz; C = approximate line of discontinuity in the growth direction of the fibres; D = syntaxial fibrous to blocky-elongate quartz exhibiting clear growth competition; E = termination of syntaxial fibrous quartz in top half of sample; F = blocky quartz; G = isolated region of fibrous quartz; H = later subhedral blocky prismatic quartz and calcite.*

The textural variation between fibrous and blocky quartz in the Nugget vein can also be observed at the macroscale in the field (Fig. 9).
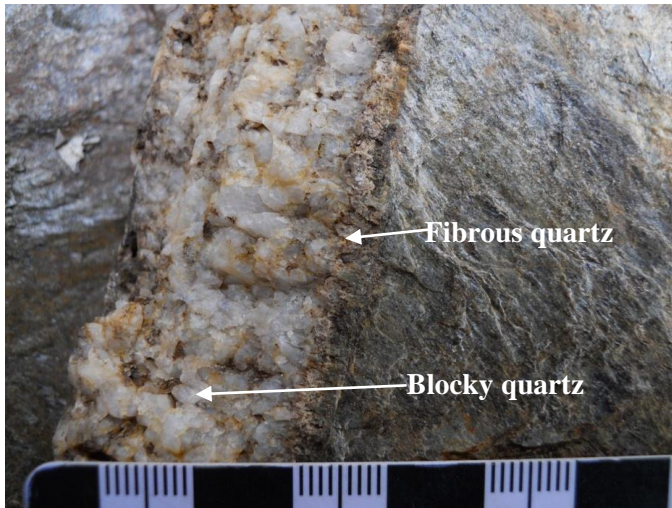
Figure 9: Field photograph of the Nugget vein, showing a cross-section from right to left through foliated wallrock, early fibrous quartz associated with sulphides, and later milky blocky quartz. Photo courtesy of M. Allan.

5.1.2 Sheba Vein

Sample MA-11-SH3 from the Sheba vein (Fig. 10) is the second of the two samples that contain fibrous quartz, but differs substantially from MA-11-NG4. In this sample there are two clear zones of growth – a region of fibrous grains with, on either side, medium to coarse-grained subhedral to anhedral blocky quartz with extensive microinclusions. The quartz fibres are generally consistent in width throughout the vein, and have no apparent evidence of growth competition between adjacent crystals, or continuity with the wallrock. An inclusion band of wallrock muscovite is present to the left of the fibrous grains.
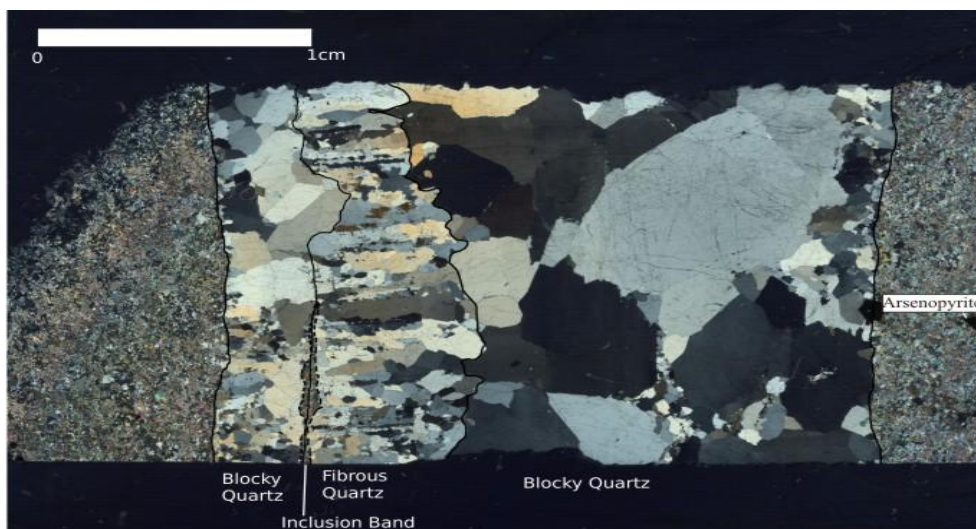
Figure 10: XPL photomicrograph of sample MA-11-SH3. In the vein, a region of fibrous quartz is flanked by two inclusion-rich blocky quartz zones. Euhedral grains of arsenopyrite are associated with the wallrock and the vein wall.

18

5.2 Discussion and Interpretation

The variety of vein textures and microstructures observed in the different samples can serve as kinematic tracers for the evolution of the veins. As mentioned in Chapter 2, the crystal morphology is largely controlled by the balance between opening rate of the vein aperture and growth rate of the vein minerals.

Most vein samples are dominated by blocky quartz, indicating continuing nucleation after the initial vein formation, most likely due to silica oversaturation (Oliver and Bons, 2001). Thus, the predominantly narrow, intergrown blocky veins which are seen in most of the samples are the result of vein dilation rates exceeding crystal growth, allowing the quartz to grow into free space (Hilgers et al., 2001). The bands of finer quartz at the vein wall may be the product of rapid crystallization of the silica in contact with the wall; or may result from higher growth competition along the wall, where many nucleation sites were available after initial fracturing of the host rock. The more elongate textures observed in sample MA-11-DY1, from the Dysle vein, can be determined from hand samples of the rock to be the product of secondary infilling of vugs.

5.2.1 Fibrous Veins

Of the two veins containing fibrous quartz, sample MA-11-NG4 (Fig. 8) is the most texturally complex, as described above. Textural similarities exist between quartz in the wallrock and adjacent vein quartz fibres, with many fibres of approximately equal width to the quartz laminae in the host rock. In addition, muscovite laminae continue into the vein as inclusions trails. These relationships between the vein and wallrock indicate the use of the wallrock quartz as a crystallographic 'template' for the vein growth, with possible epitaxial overgrowth from the wall into the vein.

These interpretations are consistent with the formation of either syntaxial or ataxial veins. The lack of a median line would appear to suggest ataxial growth; however, the presence of growth competition and the widening of fibres into more elongate-blocky grains is more consistent with the formation of fibrous to elongate-blocky quartz in syntaxial veins, through a crack-seal process (Oliver and Bons, 2001, Hilgers and Urai, 2002).

The presence of blocky quartz surrounding an isolated region of fibrous quartz in the top half of the section requires more complex interpretations. The blocky quartz would apparently require a greater rate of vein opening than dictated by the elongate crystals. Thus,

there is the contradiction of two textures requiring different conditions, apparently forming at the same time alongside each other. This may possibly be explained, if the isolated region of fibrous quartz was at one time attached to the rest of the fibres, and was separated by a later fracturing event that allowed the blocky quartz to crystallize around it. Multiple fractures, both parallel and perpendicular to the existing vein, may have allowed the quartz-forming fluid to flow around the larger, more resistant elongate-blocky grains. It is difficult to make a determination without seeing the wallrock at the other side of the vein.

Sample MA-11-SH3 also contains fibrous quartz textures (Fig. 10), which may be consistent with either antiaxial or ataxial growth, as the relationship between the fibres and wallrock is obscured by the blocky quartz separating the fibrous region from the vein wall. However, the absence of a clearly defined median line, and the lack of evidence for growth competition, suggest ataxial growth as the most likely mechanism (Oliver and Bons, 2001). As described in Chapter 2, ataxial or stretched crystals are columnar fibres that cross the vein, connecting grains in the wall rock (Hilgers and Sindern, 2005). The interpretation of this texture is a slow growth of quartz crystals from one wall to the other, at approximately the same rate as the vein dilation.

This differs significantly from the development of the rest of the vein. The regions of blocky quartz flanking the fibres are interpreted to have developed as part of one fracturing event, with the vein opening up on either side of the pre-existing fibrous grains. This timing is supported by the presence of an inclusion band adjacent to the fibrous grains, indicating that at one time the fibres were in contact with the wallrock.

5.2.2 Structural Interpretations

Orogenic gold deposits tend to be structurally hosted, associated with second or higher order faults and restricted to the brittle-ductile transition zone (McCuaig and Kerrich, 1998). As discussed above, the gold-bearing quartz veins in the Klondike are controlled at all scales by F_4 fold axial surface fractures, and are thus interpreted as having occurred late in or following D_4 deformation (MacKenzie et al., 2008).

As D_4 post-dates the initial stages of uplift through the brittle-ductile transition in the crust (MacKenzie et al., 2008), a possible explanation is provided for the textural variation. Early stages of brittle behaviour result in episodic opening of small fractures with slow strain rates, leading to fibrous structures strongly associated with the wallrock (hence the syntaxial

growth of the elongate-blocky grains in sample MA-11-NG4, using the wallrock quartz as a crystallographic template).

Upon further uplift into a more brittle regime, the vein growth transitions into a more rapid fracturing, leading to the development of blocky, coarser quartz crystals. Fracturing in zones of weakness around the pre-existing fibrous quartz results in isolated zones of quartz fibres, such as those observed above (particularly in Fig. 8).

These interpretations are not consistent with the previously published literature on the formation of the veins, such as the statement by Chapman et al. (2010a) that vein formation appears to be from a single-stage process rather than repeated fluid pulses. The varying textures, in addition to the observed spatial association of gold and sulphide mineralization with the fibrous rather than the blocky quartz, suggest more episodic vein growth.

6.0 TRACE ELEMENTS IN OROGENIC QUARTZ VEINS

6.1 Results

Four sets of trace element data were generated by laser ablation ICP-MS: two thin section analyses, 'NG4_thin' and 'SH3_thin'; and two polished block analyses, 'NG4_thick' and 'SH3_thick'. The extended table of results can be found in Appendix III, and the locations for each of the spot analyses in Appendix II. Across these samples, the most variable and abundant trace element was Al, with measured concentrations of 40-50ppm for the thick sections and greater than 1000ppm for the thin sections. The other trace elements that consistently produced results above detection limits in all samples were Li, K and Ti. In general, most elements registered values near detection limits, and with high relative errors.

6.1.1 Thin Sections

Initial laser ablation trials on polished thin sections highlighted limitations to the generation of reliable data. Notwithstanding the relative ease of selecting inclusion-free grains, the quartz tended to spall away leaving an irregular crater. This resulted in an initial pulse of material to the ICP-MS, which tailed off abruptly as the laser ablated into the glue beneath the quartz. Within this narrow window of noisy data, it was difficult to differentiate between trace elements in quartz and surface contamination.

Consequently, the results for the thin sections were substantially more variable than the polished blocks, where it was possible to ablate in a more controlled manner, drill deeper, and obtain a relatively spike-free range of data. Apparent concentrations were more than an order of magnitude greater in the thin sections (Fig. 11), and with much larger standard errors, most likely reflecting surface contamination and uncertainties related to the shorter ICP-MS signals and uncontrolled ablation characteristics.
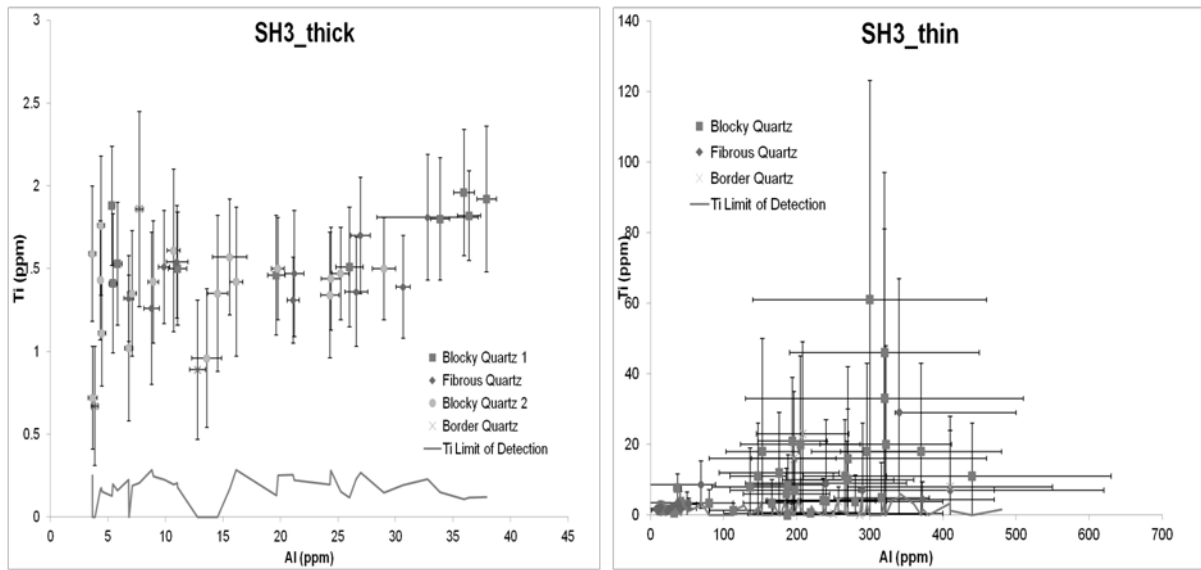
Figure 11: Graph of Ti and Al concentrations, comparing the ranges of values and relative errors for the polished blocks (left) and the thin sections (right).

The data collected from the off-cuts is considered valid, whereas the thin section data is judged unreliable and will not be used to draw any conclusions. However, the polished blocks also have certain limitations, such as the greater difficulty in selecting inclusion-free grains for ablation and the increased likelihood of surface contamination, and these must be borne in mind when interpreting the data.

6.1.2 Polished Blocks

There are limited correlations among trace elements (Fig. 12). Primarily among these, Li appears to correlate positively with Al, with an average Li/Al molar ratio of ~0.026.

The values for Ti and K are predominantly low (less than 3ppm for most Ti and less than 10ppm for most K values). The other consistent relationship is that of Ge and Al. Ge values remain mostly steady at around 0.5 – 2.5ppm, over a range of almost 40ppm Al.

SAMPLE 'NG4_Thick'   ## SAMPLE 'SH3_Thick'
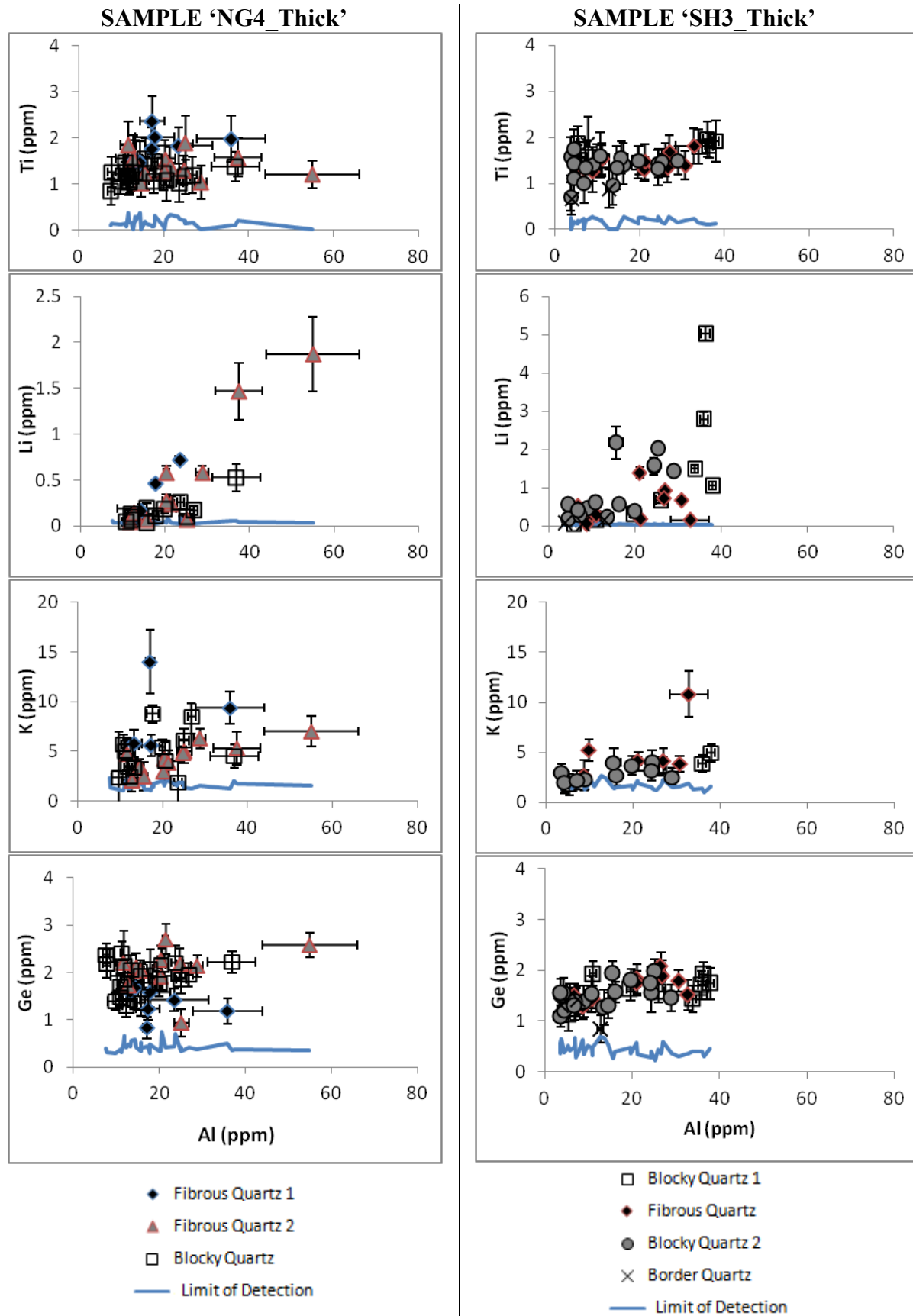
Figure 12: *Trace element correlation plots for polished blocks.*

There are also few clear observable variations among the various quartz generations. In 'NG4_thick', fibrous quartz appears to have higher average trace element concentrations than the blocky quartz, but this trend does not hold for any of the other sections.

6.2 Discussion

The limited trends that could be identified from the laser ablation analysis of samples MA-11-SH3 and MA-11-NG4 are for the most part consistent with previous studies. The abundance of Al relative to other trace elements is explained by the ease with which Al^{3+} can substitute for Si^{4+} in the quartz crystal lattice, due to their similar ionic radii; in addition to the common occurrence of Al in the Earth's crust (Rusk et al., 2008, Götze, 2009). The correlation between Li and Al for many of the quartz grains has also been documented in literature, and attributed to charge compensation by Li^{+} accompanying the tetrahedral substitution of $[AlO_4]^{-}$ in $[SiO_4]^{0}$ sites (Landtwing and Pettke, 2005, Allan and Yardley, 2007). The molar Li/Al ratio of ~0.026 was significantly lower than those reported in previous studies – across several different samples from both high and low temperature deposits, Rusk et al. (2011) found molar Li/Al ratios between 0.125 and 0.5. The low Li/Al ratio suggests that H^{+} may be the dominant charge-balancing cation for $[AlO_4]^{-}$ substitutional sites.

As discussed in Chapters 2 and 3, correlations have been established in nature between the Ti concentration of quartz and its temperature of crystallization, and have been quantified experimentally above 600°C (Wark and Watson, 2006, Allan and Yardley, 2007). Wark and Watson (2006) developed a geothermometer allowing the determination of quartz crystallization temperature from the concentration of Ti in quartz, assuming the fluid is in equilibrium with rutle, using the following equation:

$$T(°C) = \frac{-3765}{\log(X_{qtz}^{Ti}) - 5.69} - 273$$

(X_{qtz}^{Ti}) is the concentration of Ti in quartz (in parts per million by weight). The application of this geothermometer to the trace element data produces a range of crystallization temperatures between 369°C and 435°C, with an average crystallization temperature of 407°C. Orogenic gold deposits are typically found in the 300-400°C range, although they can form at 220° – 600°C (Groves et al., 2003). This suggests that the trace element values are consistent with the expected range of values from an orogenic quartz system. Thus, although

the Wark and Watson TitaniQ geothermometer is only calibrated for temperatures above 500°C, it produces a geologically sensible range of temperature for the Klondike veins.

Rusk et al. (2008) also examined trace elements in quartz, comparing the concentrations of Ti in high-temperature deposits (<10 to ~170ppm) and low-temperature deposits (below detection) with Al concentrations (Fig. 13a). Following this scheme, these samples, sources from low-temperature orogenic veins, would be expected to have very low Ti concentrations. This is indeed the case, with the majority of Ti falling below 3ppm, very close to the detection limit (Fig. 13b).
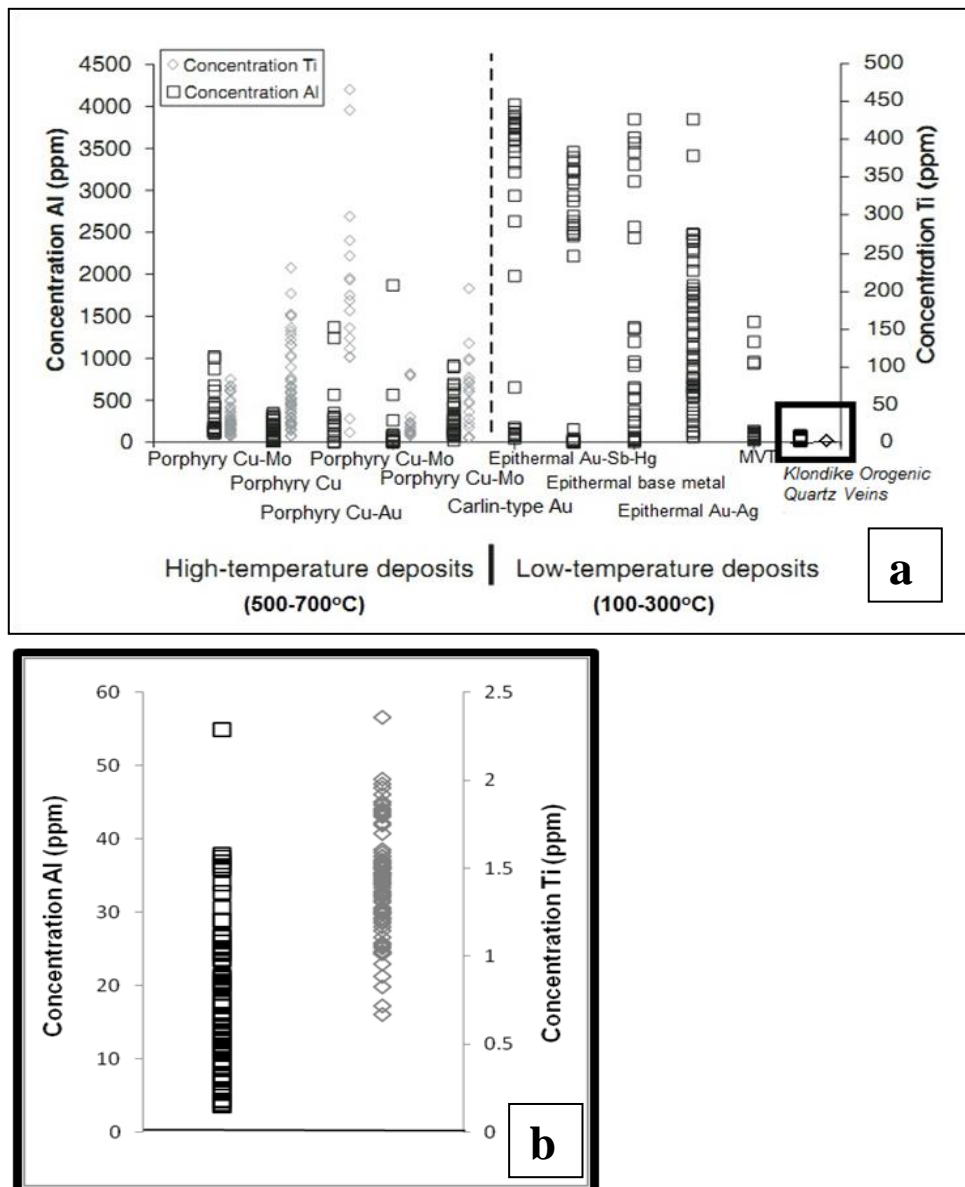
Figure 13. a: Concentrations measured in quartz from various ore deposits. The polished block results from this study have been plotted at lower right (boxed area). Modified from Rusk et al. (2008). b: Expanded plot of Ti (grey diamonds) and Al (black squares) concentrations from Klondike orogenic quartz vein samples.

The relationship that was observed between Ge and Al does not appear to have been discussed in the existing literature. A potential substitution is Ge^{4+} for Si^{4+}. This relationship could be investigated further, although it is important to remember that the detected concentrations of Ge are very low, less than 3ppm, and as such may not be entirely accurate.

The textural variations within samples MA-11-NG4 and MA-11-SH3 are discussed above. This study sought to test the hypothesis that the different conditions of formation interpreted for each quartz type would be reflected in the trace element chemistry. However, there were no statistical differences in the trace element concentration between the different textures.

This leads to the conclusion that the physical and chemical conditions of quartz growth did not vary significantly for the different textural domains throughout the development of the veins, allowing the fluid to remain in equilibrium with the host rock. Thus, the fibrous and blocky textures likely represent a fairly narrow range of fluid compositions and temperatures.

To test the validity of these observations, similar studies should be carried out for more of the samples from different veins. In this way, the variation over a wider range of textures could be compared. To avoid the limitations encountered with thin sections, any future analyses should involve polished thick sections (100-200μm), as opposed to standard polished thin sections. A detailed fluid inclusion study for these veins might also address the formation conditions and fluid chemistry of the vein generations, and reveal more subtle differences.

7.0 CONCLUSION

This thesis has examined a series of samples from gold-bearing orogenic quartz veins in the Klondike District. Vein structures and textures were analyzed, and trace element concentrations were measured.

Examining the quartz textures and structures allowed the veins to be grouped into two broad categories – the blocky veins produced by a single fracturing event with dilation rate exceeding the rate of quartz growth into open space; and the elongate-blocky to fibrous veins that record multiple events of opening, with the average rate of opening equal to the average rate of quartz growth. These textural variations would appear to indicate varying physical and chemical conditions for the formation of the veins, likely due to changing crustal levels, progressing through the brittle-ductile transition within the crust, and increased strain rates.

The lack of significant variation in trace element signatures suggests there was little difference between the conditions of formation of the different quartz textures. Thus, the textural differences are likely a product of structural rather than geochemical variations.

From the trace element data, it was possible to conclude that Al is the most abundant element in quartz, and that orogenic quartz veins contain generally low concentrations and variability of trace elements when compared with higher temperature hydrothermal and magmatic systems. A correlation between Al and Li is consistent with other literature on the subject, although the average molar Li/Al ratio of 0.026 was lower than expected; while a possible correlation between Ge and Al may require further investigation.

Evidently, there are limitations to this data, such as the high variability in results, the contrast between the values for thin sections and polished blocks, and the large standard errors. Further studies building on this work should focus on thicker blocks rather than thin sections, and trace element data should be collected for the blocky veins that contain no elongate grains, to allow more extensive comparisons.

On the side of the textures, further analysis is also warranted – other samples from the same veins could assist in constraining the structural variations, particularly in unravelling the opening history of the Nugget vein. Finally, of substantial interest for mineral exploration is the need to determine the timing of gold mineralization in the veins, as part of the ongoing process of characterizing the structural development of vein-hosted lode gold deposits in the Klondike.

<div style="text-align: center;">**REFERENCES CITED**</div>

Allan, M. M., & Yardley, B. W. D. (2007). Tracking meteoric infiltration into a magmatic-hydrothermal system: A cathodoluminescence, oxygen isotope and trace element study of quartz from Mt. Leyshon, Australia. *Chemical Geology, 240*(3-4), 343-360.

Beurlen, H., Muller, A., Silva, D., & Da Silva, M. R. R. (2011). Petrogenetic significance of LA-ICP-MS trace-element data on quartz from the Borborema Pegmatite Province, northeast Brazil. *Mineralogical Magazine, 75*(5), 2703-2719.

Chapman, R. J., Mortensen, J. K., Crawford, E. C., & Lebarge, W. (2010). Microchemical studies of placer and lode gold in the Klondike district, Yukon, Canada: 1. Evidence for a small, gold-rich, orogenic hydrothermal system in the Bonanza and Eldorado creek area. *Economic Geology, 105*(8), 1369-1392.

Chapman, R. J., Mortensen, J. K., Crawford, E. C., & Lebarge, W. P. (2010). Microchemical studies of placer and lode gold in the Klondike district, Yukon, Canada: 2. Constraints on the nature and location of regional lode sources. *Economic Geology, 105*(8), 1393-1410.

Donovan, J. J., Lowers, H. A., & Rusk, B. G. (2011). Improved electron probe microanalysis of trace elements in quartz. *American Mineralogist, 96*(2-3), 274-282.

Dubé, B., & Gosselin, P. (2007). Greenstone-hosted quartz-carbonate vein deposits. In: Goodfellow, W.D. (ed.) Mineral Deposits of Canada: A Synthesis of Major Deposit-Types, District Metallogeny, the Evolution of Geological Provinces, and Exploration Methods. *Geological Association of Canada, Mineral Deposits Division, Special Publication 5,* 49-73.

Gabrielse, H., Murphy, D.C., & Mortensen, J.K. (2006). Cretaceous and Cenozoic dextral orogen-parallel displacements, magmatism, and paleogeography, north-central Canadian Cordillera. In: Haggart, J.W., Enkin, R.J., Monger, J.W.H. (eds) Paleogeography of the North American Cordillera: Evidence For and Against Large-Scale Displacements. *Geological Association of Canada, Special Paper 46*, 645-659.

Goldfarb, R.J., Baker, T., Dubé., B., Groves, D.I., Hart, C.J.R., & Gosselin, P. (2005). Distribution, character, and genesis of gold deposits in metamorphic terranes. In: Hedenquist, J.W., Thompson, J.F.H., Godlfarb, R.J., Richards, J.P. (eds) Economic Geology 100th Anniversary Volume, 407-450.

Götze, J. (2009). Chemistry, textures and physical properties of quartz - geological interpretation and technical application. *Mineralogical Magazine, 73*(4), 645-671.

Götze, J., Plötze, M., Graupner, T., Hallbauer, D., & Bray, C. (2004). Trace element incorporation into quartz: A combined study by ICP-MS, electron spin resonance, cathodoluminescence, capillary ion analysis, and gas chromatography. *Geochimica Et Cosmochimica Acta, 68*(18), 3741-3759.

Groves, D. I., Goldfarb, R. J., Gebre-Mariam, M., Hagemann, S. G., & Robert, F. (1998). Orogenic gold deposits: A proposed classification in the context of their crustal distribution and relationship to other gold deposit types. *Ore Geology Reviews, 13*(1-5), 7-27.

Groves, D., Goldfarb, R., Robert, F., & Hart, C. (2003). Gold deposits in metamorphic belts: Overview of current understanding, outstanding problems, future research, and exploration significance. *Economic Geology and the Bulletin of the Society of Economic Geologists, 98*(1), 1-29.

Hilgers, C., & Sindern, S. (2005). Textural and isotopic evidence on the fluid source and transport mechanism of antitaxial fibrous microstructures from the Alps and the Appalachians. *Geofluids, 5*(4), 239-250.

Hilgers, C., & Urai, J. L. (2002). Microstructural observations on natural syntectonic fibrous veins: implications for the growth process. *Tectonophysics, 352*(3-4), 257-274.

Hilgers, C., Koehn, D., Bons, P. D., & Urai, J. L. (2001). Development of crystal morphology during unitaxial growth in a progressively widening vein: II. Numerical simulations of the evolution of antitaxial fibrous veins. *Journal of Structural Geology, 23*(6-7), 873-885.

Jia, Y. F., Kerrich, R., & Goldfarb, R. (2003). Metamorphic origin of ore-forming fluids for orogenic gold-bearing quartz vein systems in the North American Cordillera: Constraints from a reconnaissance study of delta N-15, delta D, and delta O-18. *Economic Geology and the Bulletin of the Society of Economic Geologists, 98*(1), 109-123.

Knight, J. B., Mortensen, J. K., & Morison, S. R. (1999). Lode and placer gold composition in the Klondike district, Yukon Territory Canada: Implications for the nature and genesis of Klondike placer and lode gold deposits. *Economic Geology and the Bulletin of the Society of Economic Geologists, 94*(5), 649-664.

Landtwing, M. R., & Pettke, T. (2005). Relationships between SEM-cathodoluminescence response and trace-element composition of hydrothermal vein quartz. *American Mineralogist, 90*(1), 122-131.

Lowey, G. W. (2006). The origin and evolution of the Klondike goldfields, Yukon, Canada. *Ore Geology Reviews, 28*(4), 431-450.

MacKenzie, D. J., Craw, D., & Mortensen, J. (2008). Structural controls on orogenic gold mineralisation in the Klondike goldfield, Canada. *Mineralium Deposita, 43*(4), 435-448.

McCuaig, T., & Kerrich, R. (1998). P-T-t-deformation-fluid characteristics of lode gold deposits: evidence from alteration systematic. *Ore Geology Reviews, 12*(6), 381-453.

Mortensen, J. K. (1990). Geology and U-Pb geochronology of the Klondike district, west-central Yukon Territory. *Canadian Journal of Earth Sciences, 27*(7), 903-914.

Muller, A., Rene, M., Behr, H. J., & Kronz, A. (2003). Trace elements and cathodoluminescence of igneous quartz in topaz granites from the Hub Stock (Slavkovsky Les Mts., Czech Republic). *Mineralogy and Petrology, 79*(3-4), 167-191.

Oliver, N. H. S., & Bons, P. D. (2001). Mechanisms of fluid flow and fluid-rock interaction in fossil metamorphic hydrothermal systems inferred from vein-wallrock patterns, geometry and microstructure. *Geofluids, 1*(2), 137-162.

Ramsay, J. G. (1980). The crack-seal mechanism of rock deformation. *Nature, 284*, 135-139.

Ridley, J. R., & Diamond, L. W. (2000). Fluid chemistry of orogenic lode-gold deposits and implications for genetic models. *Reviews in Economic Geology 13,* 141-162.

Rushton, R. W., Nesbitt, B. E., Muehlenbachs, K., & Mortensen, J. K. (1993). A fluid inclusion and stable isotope study of Au quartz veins in the Klondike district, Yukon-Territory, Canada - a section through a mesothermal vein system. *Economic Geology and the Bulletin of the Society of Economic Geologists, 88*(3), 647-678.

Rusk, B. G., Lowers, H. A., & Reed, M. H. (2008). Trace elements in hydrothermal quartz: Relationships to cathodoluminescent textures and insights into vein formation. *Geology, 36*(7), 547-550.

Rusk, B. G., Reed, M. H., Dilles, J. H., & Kent, A. J. R. (2006). Intensity of quartz cathodoluminescence and trace-element content in quartz from the porphyry copper deposit at Butte, Montana. *American Mineralogist, 91*(8-9), 1300-1312.

Rusk, B., Koenig, A., & Lowers, H. (2011). Visualizing trace element distribution in quartz using cathodoluminescence, electron microprobe, and laser ablation-inductively coupled plasma-mass spectrometry. *American Mineralogist, 96*(5-6), 703-708.

Wark, D. A., & Watson, E. B. (2006). TitaniQ: A titanium-in-quartz geothermometer. *Contributions to Mineralogy and Petrology, 152*(6), 743-754.

APPENDIX I: DETAILED THIN SECTION AND ROCK DESCRIPTIONS

<u>**Sample: MA-11-AM2**</u>

Vein Mineralogy:
90% Blocky, subhedral to anhedral **quartz**. Coarse crystals predominantly containing fine quartz inclusions. Interstitial very fine quartz, likely recrystallized. Grains fine towards vein centre. Extensive microinclusions.
10% Fine-grained massive **Fe-Carbonate**. Predominantly dark orange-brown, in 2 elongate bands, 2-3mm wide, approximately parallel to vein. 1 band is near the vein centre, one at the wall-vein interface. Fine bladed calcite at edges of bands. Effervesces in dilute HCl.

Host Rock Mineralogy:
70% Medium-fine rounded-elongate **quartz**, with possible fine **feldspar.** Fines away from boundary with vein.
20% Elongate **muscovite**, foliated, with orange rims.
5% Fine **carbonate** alteration.
5% Oxidized **pyrite**, disseminated throughout wallrock and associated with vein-wall interface. Euhedral to subhedral.

Vein Textures:
The sample covers approximately half the width of a quartz vein. The vein is characterized by blocky, intergrown quartz, most likely forming in one event, with later fine recrystallization along grain boundaries.
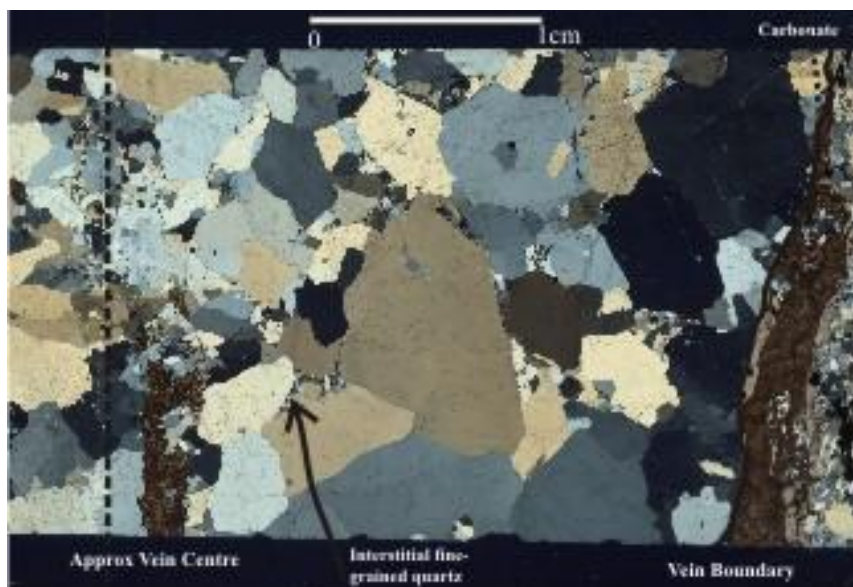
Figure 14: XPL photomicrograph of sample MA-11-AM2

<u>**Sample: MA-11-AM3**</u>

Vein Mineralogy:
90% Blocky, subrounded, anhedral intergrown **quartz**. Mildly deformed, extensive inclusions.

7%	Fine-grained **quartz**, at vein-wall interface and interstitial to the coarser, blocky quartz.
3%	Fine **muscovite**, inclusions in the blocky quartz and infilling deep fractures.

Host Rock Mineralogy:

45%	**Muscovite**, elongate, foliation approximately parallel to vein. Orange alteration rims.
33%	Fine-grained **quartz**, rounded to elongate grains, foliated. Larger fragmented grains at wall, with mica inclusions.
20%	Fine-grained **calcite** and fine **carbonate** alteration.
2%	Fine, subhedral to euhedral **pyrite**. Extensively oxidized.

Vein Textures:

The sample extends from one vein wall to within 1cm of the opposite wall. Blocky quartz decreases in size in both directions from the centre of the vein towards the wallrock, with substantially finer grains precipitating at the vein-wall boundary. The vein likely precipitated from one fracturing event, with later fine-grained recrystallization along grain boundaries.
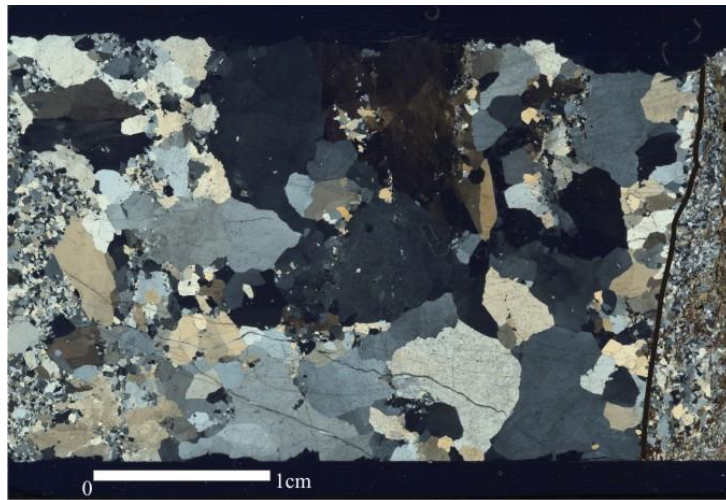
Figure 15*: XPL photomicrograph of sample MA-11-AM3.*

Sample: MA-11-DY1

Vein Mineralogy:

100%	White vuggy **quartz**, mildly deformed to undeformed. Predominantly coarse grains, elongate horizontally across vein. Anhedral to subhedral. Regions of finer interstitial recrystallized quartz. Extensive very fine inclusions in coarser grains, leading to 'dusty' look. Grains vary from >6mm to <0.5mm diameter.

Host Rock Mineralogy:

70%	Fine **muscovite** and **chlorite**, elongate, fractured, foliated. **Fe-carbonate** alteration rims.
30%	Fine anhedral **quartz**, subrounded.

Vein Textures:

The sample extends across the entire vein, with blocky to elongate-blocky quartz grains. In hand sample, the section consists of coarse, vuggy quartz, growing into space from the vein

edges. Scattered subhedral medium-grained quartz and fine interstitial recrystallized quartz likely crystallized later.
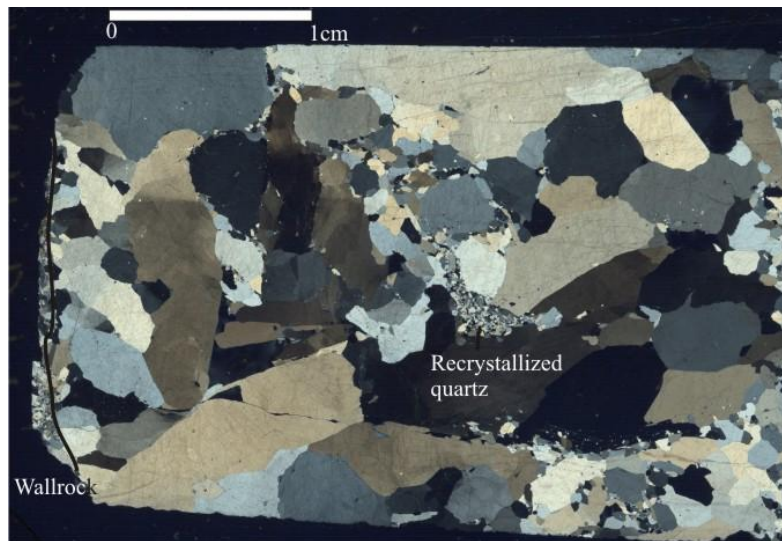
Figure 16: XPL photomicrograph of sample MA-11-DY1.

Sample: MA-11-DY2

Vein Mineralogy:
97%   Anhedral, blocky **quartz**, heavily deformed. Undulatory extinction, extensively fractured. Finer grains at wall-vein interface. Elongation of fine boundary grains in the same direction as the host rock micas.
3%   Fine **mica** inclusions at wall-vein interface.

Host Rock Mineralogy:
40%   Fine to very fine **quartz and feldspar.** Albite-twinned plagioclase, fine-grained perthite. Deformed quartz and feldspar twins.
30%   **Muscovite** and **chlorite**, fine-grained, foliated.
20%   **Iron oxide** alteration, predominantly interstitial and on grain boundaries.
10%   Coarse deformed **quartz** grains, fractures infilled with fine quartz and feldspar from the groundmass.

Vein Textures:
Vein is approximately 2-3 grains in width (~11mm), consisting of anhedral coarse intergrown blocky quartz growing across the vein, with a narrow band of fine quartz at the vein walls.
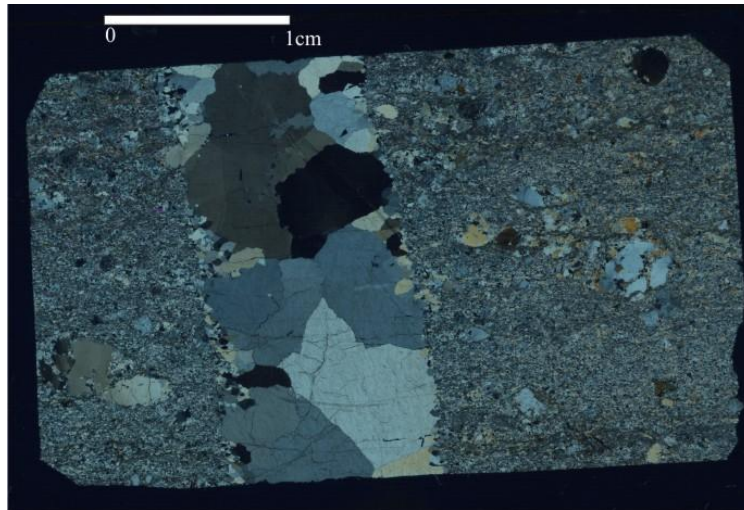
Figure 17: XPL photomicrograph of sample MA-11-DY2.

Sample: MA-11-MK2

Vein Mineralogy:

>90%   **Quartz**, intergrown equant crystals, anhedral to subhedral. Grain size varying from <0.5mm to 5mm in diameter. Deformed crystals with extensive undulatory extinction.

5%   **Pyrite**, clustered, occasional simple twinning. Extensive oxidation at rims.

<5%   Fine grained muscovite and chlorite, interstitial to quartz grains, likely wallrock inclusions.

Host Rock Mineralogy:

65%   Foliated **chlorite** and **muscovite.** Fine-grained. Abundant patchy orange alteration.

35%   Fine-grained foliated **quartz** and **feldspar**. Anhedral, subrounded. Thickness of slide leads to anomalously bright purples and blues in XPL.

Vein Textures:

Blocky quartz. Vein-wall interface cuts across mica foliation, at 60-80°. Minor overgrowth of quartz onto wallrock.
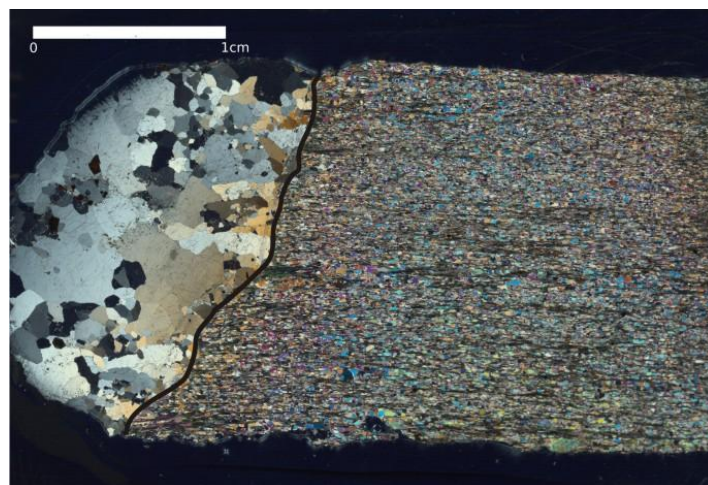
Figure 18: XPL photomicrograph of sample MA-11-MK2.

Sample: MA-11-NG2

Vein Mineralogy:
97%   **Quartz**. Elongate-blocky, highly deformed, finely fractured with 'dusty' very fine inclusions. Predominantly coarse-grained (>5mm diameter). Abundant fine interstitial quartz, possibly recrystallized. Minor orange-brown iron alteration along fractures.

3%   **Plagioclase feldspar** laths, with fine polysynthetic twinning. Restricted to one corner of section.

Host Rock Mineralogy:
75%   **Plagioclase feldspar**, medium-grained laths. Extensive deformed and fractured polysynthetic twins. Direction of elongation varies, averaging approximately at right angles to the vein wall. Intergrowth with vein quartz.

20%   Very fine-grained **quartz** and **feldspar** massive assemblage, subrounded to elongate, with orange alteration along fractures. Interstitial to coarser plagioclase laths.

5%   Fibrous **muscovite**, with extensive iron alteration. Oriented in the same direction as the plagioclase and quartz (~90° to vein wall).

<1%   Oxidized **pyrite**, euhedral, medium-grained.

Vein Textures:
The vein consists of elongate-blocky quartz growing towards the wallrock (only one wall is visible in the sample). Plagioclase laths may have grown over the boundary at a later time.
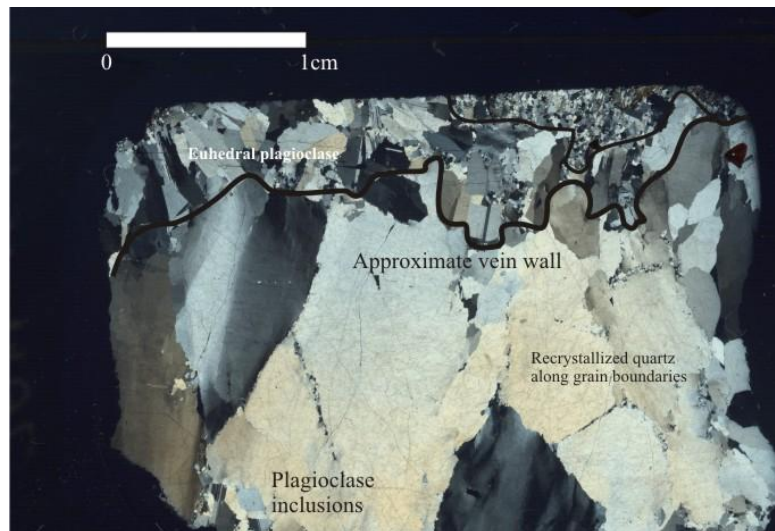
Figure 19: XPL photomicrograph of sample MA-11-NG2.

Sample: MA-11-NG4

Vein Mineralogy:
90%   **Quartz**. Fibrous, elongate-blocky, and blocky. Anhedral to subhedral, with extensive microinclusions in the blocky and elongate-blocky grains, and strong fracturing.

5%   **Muscovite**. Fine-grained wallrock inclusion trails, predominantly interstitial to the quartz fibres near the vein wall.

3%   **Calcite**. Euhedral to subhedral rhombohedral crystals, and more fine-grained aggregate. Concentrated in one region of the slide.

2%   **Pyrite**. Fine-grained (<0.5mm in diameter), subhedral , scattered throughout the vein and wallrock.

Host Rock Mineralogy:
60%   Foliated **muscovite**, very fine-grained, elongate bands. Orange-brown alteration.
40%   Fine-grained **quartz** and **feldspar**. Anhedral, intergrown, predominantly quartz.

Vein Textures:
Fibrous to elongate-blocky syntaxial quartz grows from the wallrock, in continuity with the growth direction of the wallrock quartz. Grain width increases away from the wallrock. In the top half of the slide, an isolated region of fibrous quartz is surrounded by blocky grains. Subhedral, blocky quartz grains and calcite are later replacement textures.
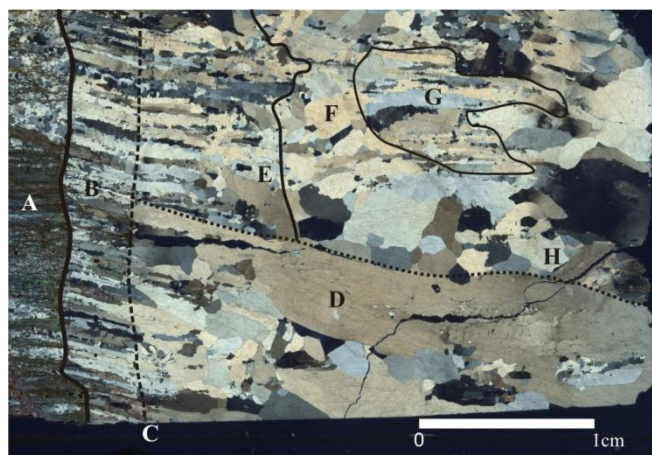
Figure 20: *XPL photomicrograph of sample MA-11-NG4. A = wallrock; B = syntaxial fibrous quartz; C = approximate line of discontinuity in the growth direction of the fibres; D = syntaxial fibrous to blocky-elongate quartz exhibiting clear growth competition; E = termination of syntaxial fibrous quartz in top half of sample; F = blocky quartz; G = isolated region of fibrous quartz; H = later subhedral blocky prismatic quartz and calcite.*

Sample: MA-11-NG5

Vein Mineralogy:
97%   White milky **quartz**. Blocky intergrowths, subhedral to anhedral grains up to 5mm in diameter. Regions of fine interstitial quartz grains, possibly recrystallized. Abundant fine inclusions in large crystals. Variably deformed.
3%   Scattered interstitial **muscovite**, host rock inclusions, most abundant near vein-wall interface.

Host Rock Mineralogy:
80%   **Quartz** and **feldspar** fine-grained assemblage. Anhedral, foliated, extensive simple and albite twinning.
20%   **Muscovite.** Elongate, predominantly in feathery folia. Orange-brown rims. ~15% of muscovite present as non-oriented grains contained within the quartz/feldspar folia.

Vein Textures:
Intersection of two veins, marked by a region of strongly deformed quartz with abundant inclusions. Jagged grain boundaries and recrystallization present throughout sample. Coarse-grained vuggy quartz present in hand sample.
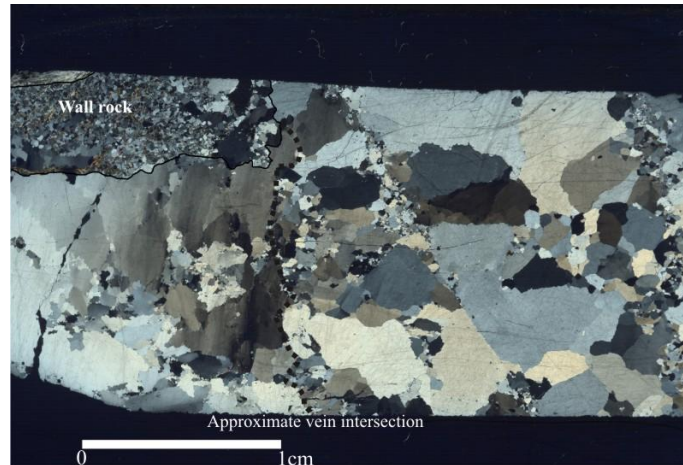
Figure 21: XPL photomicrograph of sample MA-11-NG5. Dotted line indicates approximate intersection area of the two veins.

Sample MA-11-OR1

Vein Mineralogy:
>99%   **Quartz.** Anhedral blocky quartz stretching across entire width of vein. Deformed, oriented approximately perpendicular to vein flow direction. Extensively fractured. Anhedral, fine grained quartz at vein-wall interface, <0.5 to 5mm in diameter.
<1%   **Muscovite** and **chlorite**, fine-grained, infilling fractures in quartz.

Host Rock Mineralogy:
35%   Fine-grained **quartz**, with possible very fine **feldspar.** Rounded, anhedral crystals.
30%   Elongate **chlorite**, oriented ~45° to vein. Fine-grained, low order interference colours.
20%   **Muscovite**, fine-grained, elongate, oriented.
10%   **Actinolite?** Altered, elongate, bladed to feathery, dark brown. Possible amphibole cleavages observable. Coarse-grained.
5%   Coarse to fragmented **quartz**, deformed. Subrounded to elongate/elliptical grains, possibly associate with the vein.
      Abundant brown-black alteration throughout host rock. Iron alteration along grain boundaries, fractures, and the vein-wall interface.

Vein Textures:
Vein is predominantly one-grain wide, growing across the vein, likely in one event. Fine-grained quartz at the vein-wall interface precipitated first. Mica-filled fractures cut continuously across both the fine-grained boundary quartz and the massive blocky quartz.
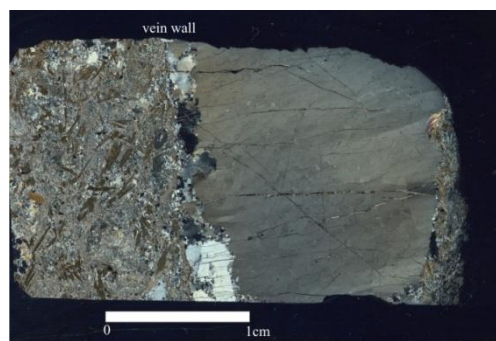
Figure 22: XPL photomicrograph of sample MA-11-OR1.

Sample: MA-11-SH3

Vein Mineralogy:

>95% **Quartz.** Region of elongate, fibrous grains and sets of fine grains forming elongate paths, flanked by anhedral, blocky intergrown quartz. Blocky quartz contains extensive microinclusions trails.

5% Interstitial fine-grained **muscovite** and **talc**, both disseminated and forming an inclusion band parallel to the fibrous-blocky quartz interface.

<1% **Arsenopyrite**, euhedral to subhedral, associated with both edges of the vein. Oxidized on rims and face, one grain completely replaced fine-grained talc.

Host Rock Mineralogy:

35% **Chlorite** and **muscovite**, mildly foliated, stubby elongate grains. Orange/brown alteration rims.

30% Anhedral **quartz**, fine-medium grained.

20% Fine grained **talc**.

15% Subhedral **plagioclase** laths, concentrated in one area.

<1% Euhedral to subhedral **arsenopyrite**. One crystal overprints vein-wall interface.

Vein Textures:

Region of fibrous, antitaxial quartz, flanked by blocky quartz. Blocky quartz fines rapidly at vein wall. Fine recrystallized quartz interstitial to blocky grains.
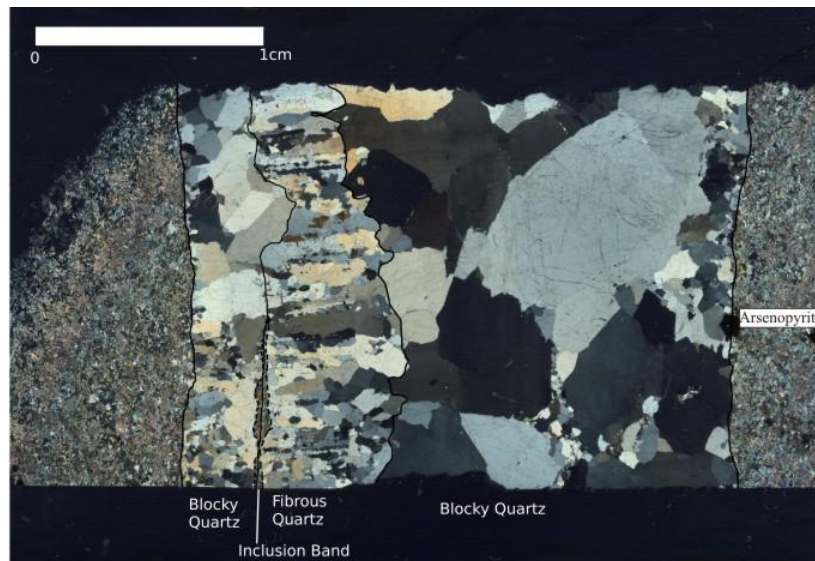
Figure 23: XPL photomicrograph of sample MA-11-SH3.

Sample: MA-11-VG2

Vein Mineralogy:

>99% Vuggy, blocky **quartz**. Highly fractured, subhedral to anhedral. Medium-grained at the centre to fine-grained at the walls. Finer-grained quartz inclusions. No interstitial mica inclusions.

<1% **Magnetite?** Sulphide grain <0.5mm in diameter. Moderate reflectance, highly oxidized rims. Subhedral.

Host Rock Mineralogy:
40%   Fine-grained **quartz** and **feldspar.**
35%   Foliated **muscovite** (±**chlorite**). Fine-grained, elongate.
20%   **Quartz**. Fractured, anhedral, fine- to medium-grained.
15%   **Plagioclase**. Medium-grained, polysynthetic and simple twinning. Extensive sericite alteration.

Abundant iron alteration throughout the host rock, concentrated near the vein and fractures.

Vein Textures:
The vein is approximately 3-4 grains across, with coarsest grains in the centre and very fine grains at the edges. Boundary is mostly well-defined, although there is one instance of a possible lens of vein quartz extending into the wall rock. Vein cuts the foliation of the micas at an angle of approximately 50-60°.
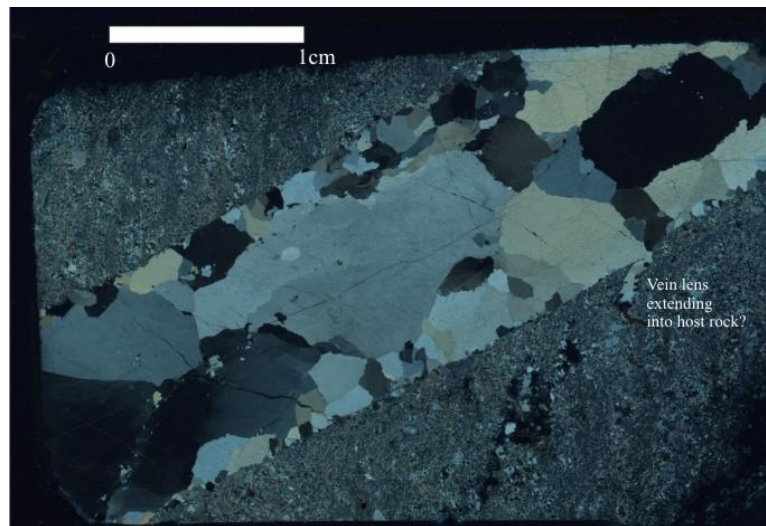
Figure 24*: XPL photomicrograph of sample MA-11-VG2.*

Sample: MA-11-VL2

Vein Mineralogy:
85%   **Quartz**. Blocky, anhedral, heavily deformed with undulatory extinction, fractured.
15%   **Feldspar**. Euhedral plagioclase laths with albite twinning and minor antiperthite. Also finer grained anhedral crystals. Strongly altered, 'dusty' with extensive fine-grained carbonate and clay alteration (mild effervescence of hand sample in dilute HCl). Cream to beige-coloured in hand sample.

Host Rock Mineralogy:
60%   Fine-grained **quartz** and **feldspar** intergrowth, anhedral. Rounded quartz inclusions present within larger feldspar grains.
<40% **Muscovite**, fine-to medium-grained, subhedral, foliated, oriented around quartzofeldspathic assemblage. Predominantly pleochroic green, distinguished from chlorite by second order birefringence.
<1%   **Pyrite**, euhedral, fragmented. Associated with vein wall, on both sides of vein.

Vein Textures:
The vein is approximately 1-2 quartz grains (5-8mm) in diameter. Euhedral feldspar laths appear to have grown onto the blocky quartz of the vein from the wall, leading to a loss of definition of the vein boundary. Extensive carbonate and possible clay alteration are evidence of later, shallower processes.
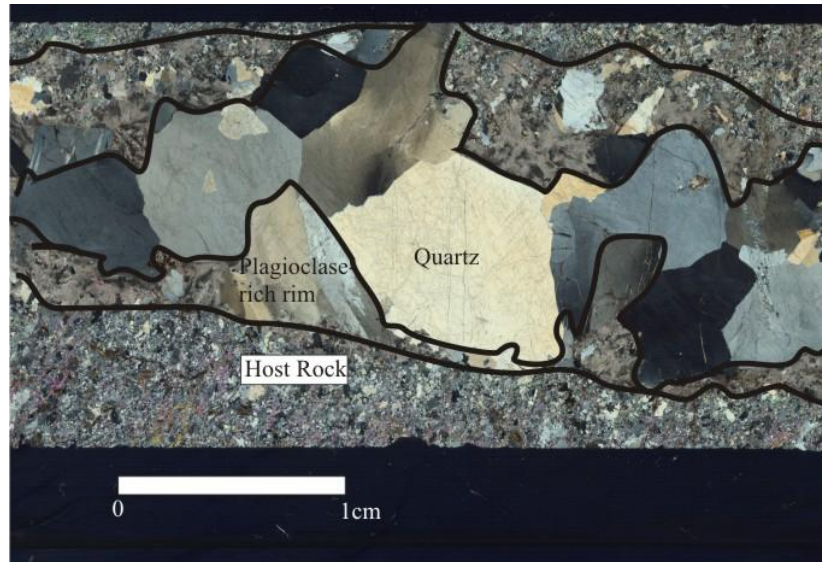
Figure 25: XPL photomicrograph of sample MA-11-VL2

APPENDIX II: LOCATIONS FOR LASER ABLATION SPOT ANALYSES

42

Thin Sections
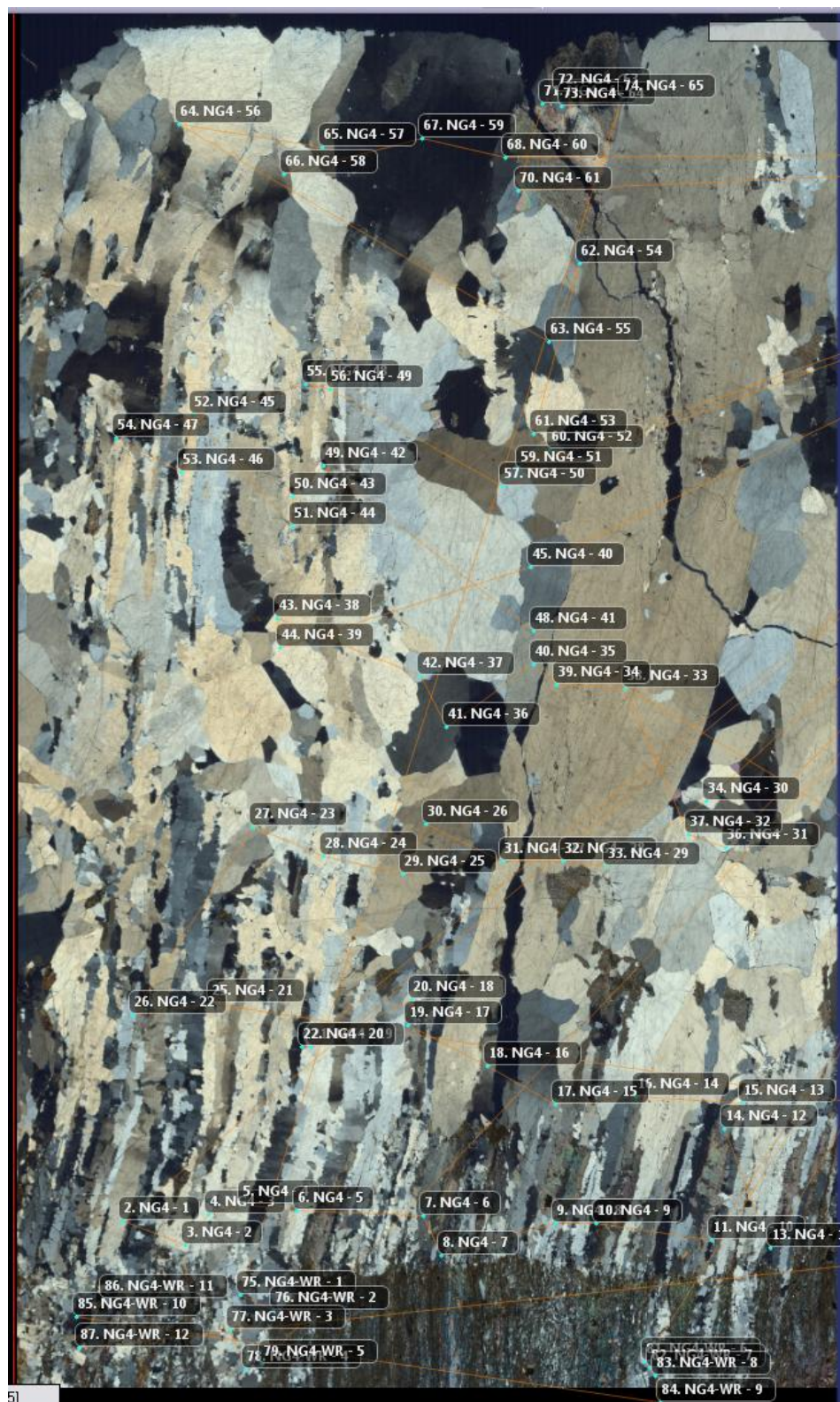
Figure 26: Labelled locations of spot analyses for 'NG4_Thin'.
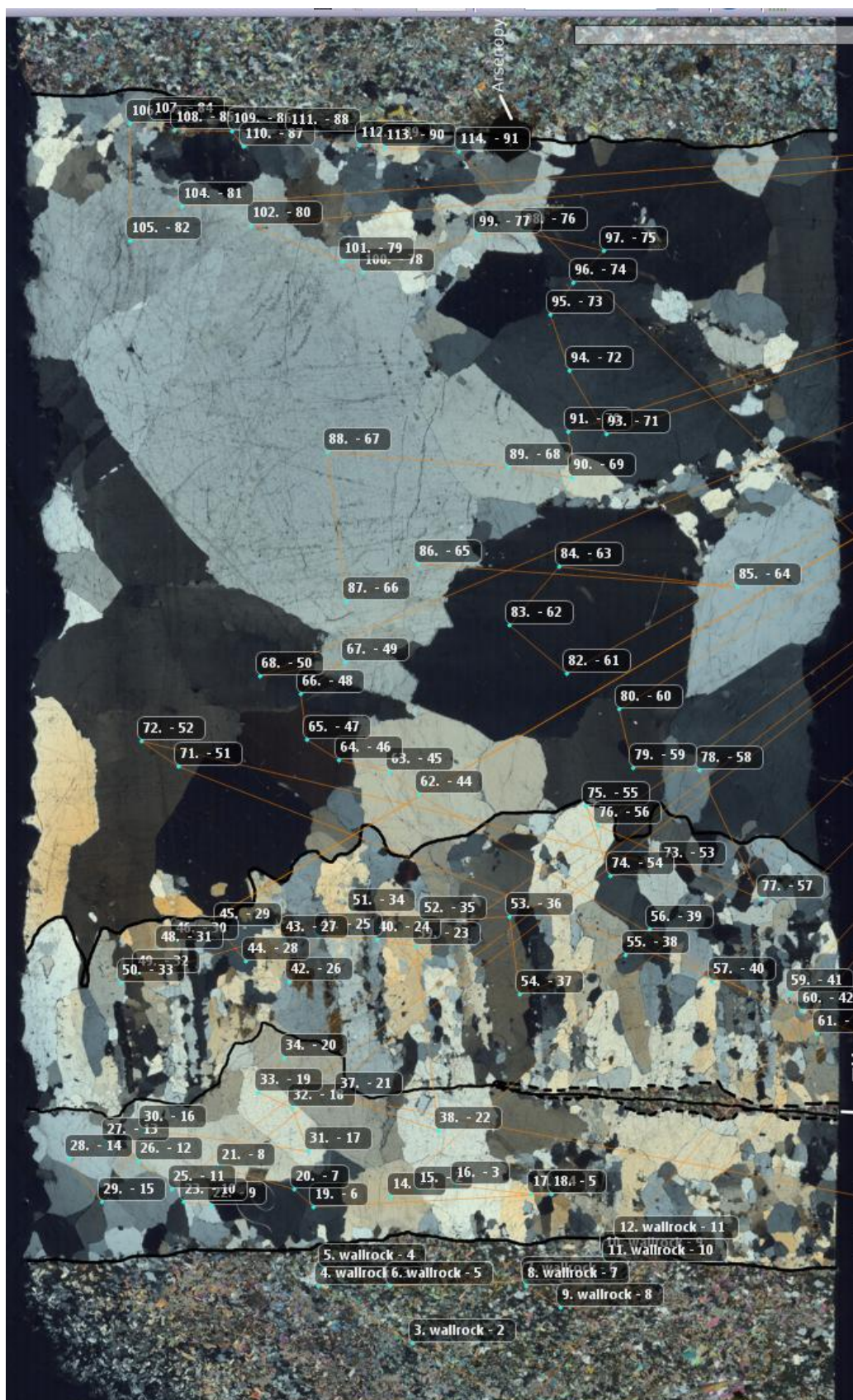
Figure 27: Labelled locations of spot analyses for 'SH3_Thin'.

Polished Blocks
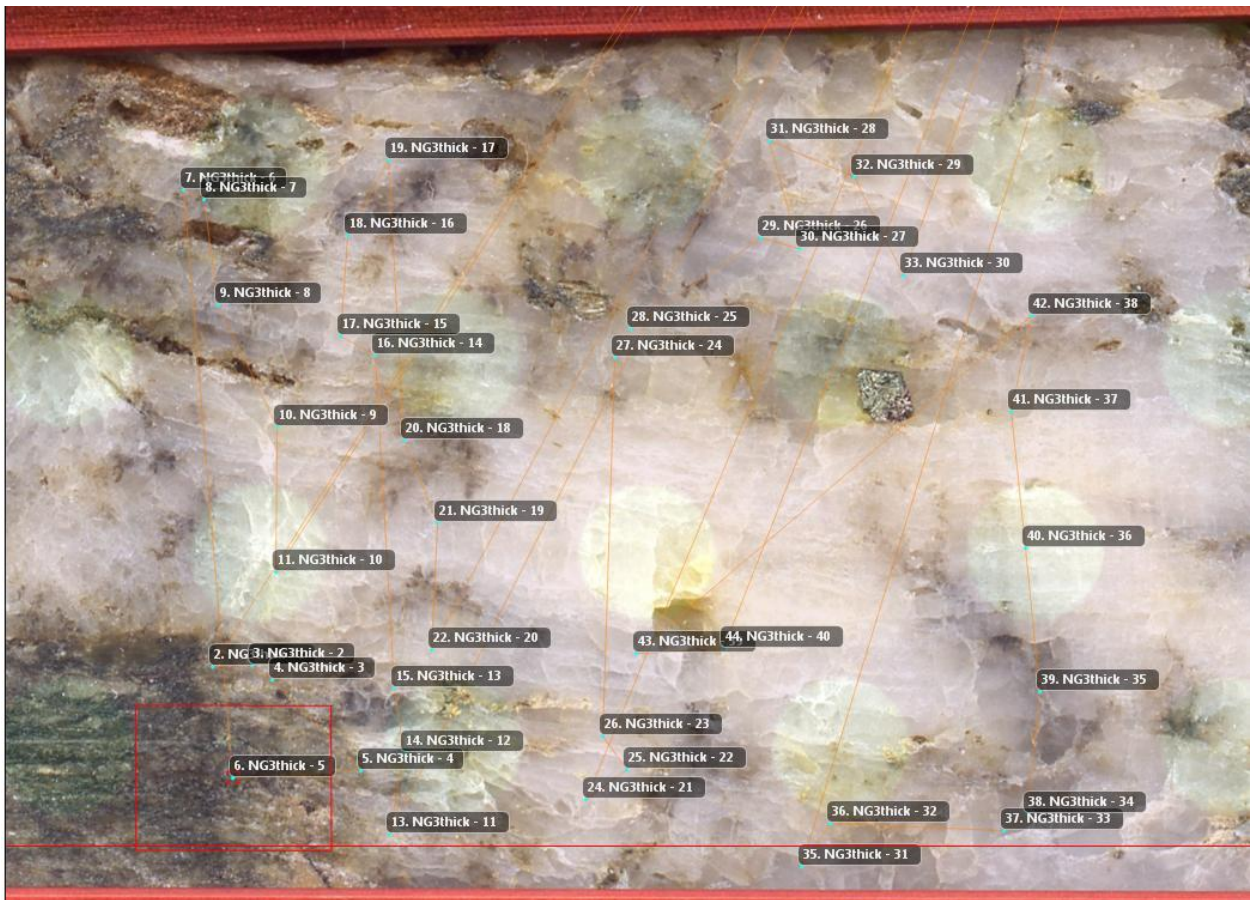
Figure 28: Labelled locations of spot analyses for 'NG4_Thick'.

Figure 29: Labelled locations of spot analyses for 'SH3_Thick'.

Table 3*: Sample 'NG4_Thin'. 'bd'= below detection limits.*

	Sample Number	Li7		Na23		Al27		K39		Ca43		Ti47		Fe57	
		(ppm)	2SE (ppm)	(ppm)	2SE (ppm)	(ppm)	2SE (ppm)	(ppm)	2SE (ppm)	(ppm)	2SE (ppm)	(ppm)	2SE (ppm)	(ppm)	2SE (ppm)
BCR Standard	BCR_Standard_1	17.98	0.48	45120	320	143100	1700	32440	300	91600	1700	26270	300	95500	560
	BCR_Standard_2	17.75	0.46	45090	290	143600	1700	32240	260	91800	1600	26240	310	98350	730
	BCR_Standard_3	17.08	0.47	45320	280	144900	1800	32160	250	90600	1500	26020	330	102790	680
NIST Standard	G_NIST612_1	41.63	0.62	104800	1600	11160	150	69.7	1.6	84000	1300	43.5	1.1	52.9	1.9
	G_NIST612_2	42.31	0.47	104200	1200	11330	160	65.52	0.91	86900	1400	44.7	1.3	51.3	1.8
	G_NIST612_3	42.27	0.72	104300	1500	11020	170	65.3	1.1	85200	1300	44.7	1.4	49.5	1.9
	G_NIST612_4	41.51	0.68	102600	1200	11070	190	65.6	1.1	84900	1400	44.1	1.6	50.3	2.2
	G_NIST612_5	41.93	0.82	103000	2300	11110	230	66.9	1.5	83600	1800	43.6	1.4	50	2.2
	G_NIST612_6	41.76	0.75	102200	1500	11190	160	67.2	1.3	84700	1200	43.6	1.2	49.8	1.8
	G_NIST612_7	42.48	0.66	105000	1300	11170	150	66.4	1.4	85200	1100	43.4	1.4	51.3	1.8
	G_NIST612_8	41.81	0.68	103200	1400	11220	130	66.1	1.1	84500	1100	44.5	1.1	50.8	2
	G_NIST612_9	41.98	0.68	105500	1700	11120	160	66.5	1.2	85800	1300	44	1.3	52.6	1.9
Fibrous Quartz 1	Vein_Quartz_1	8	19	2400	2100	3900	1400	2800	2500	36000	65000	73	49	2700	1600
	Vein_Quartz_2	0.25	0.32	22	10	17.8	2.9	bd	12	bd	290	1.24	0.87	20.2	9.9
	Vein_Quartz_3	bd	4.1	390	210	159	45	bd	280	1800	7200	30	23	410	250
	Vein_Quartz_4	5	17	590	540	340	130	bd	530	20000	29000	23	27	760	890
	Vein_Quartz_5	0.42	0.53	83	21	34.9	9.9	bd	25	bd	590	1.6	1.5	20	24
	Vein_Quartz_6	33	16	370	400	2400	1600	bd	630	8100	9900	bd	9.1	2200	2400
	Vein_Quartz_7	bd	6.2	820	760	680	430	bd	470	5000	6800	240	470	100	890
	Vein_Quartz_8	3	1.3	bd	42	104	20	bd	230	bd	1600	bd	2.3	640	710
	Vein_Quartz_9	6.9	4.8	2100	3300	590	360	bd	360	11000	12000	bd	22	80	500

	Vein_Quartz_10	15.4	6.2	120	280	295	79	bd	380	60000	12000	bd	24	230	470
	Vein_Quartz_11	2.1	2.9	720	610	1500	1200	280	170	1800	5600	bd	13	1240	840
Fibrous Quartz 2	Vein_Quartz_12	2.8	3.9	290	140	207	35	240	250	12500	6700	bd	5.2	bd	170
	Vein_Quartz_13	9.6	6.9	410	180	142	34	250	230	9400	4800	19	23	120	180
	Vein_Quartz_14	bd	4.1	370	240	214	93	39	44	bd	2500	34	31	290	510
	Vein_Quartz_15	bd	3.8	780	600	220	100	370	400	10300	8500	2.8	4.7	bd	270
	Vein_Quartz_16	1.5	4.8	230	330	270	110	60	280	2600	7800	0.8	5.5	bd	240
	Vein_Quartz_17	bd	4.4	700	250	460	110	180	210	3200	7600	bd	5.3	1140	540
	Vein_Quartz_18	bd	1.4	750	300	240	210	230	190	bd	2400	24	34	900	1000
	Vein_Quartz_19	4.4	6.9	720	290	231	53	bd	280	bd	7900	bd	12	290	200
	Vein_Quartz_20	9.2	8.6	850	330	216	72	150	240	4000	7900	bd	12	200	160
	Vein_Quartz_21	0.64	0.47	81	30	14.8	3.3	77	27	bd	530	bd	0.94	13	19
	Vein_Quartz_22	8.4	4.5	660	260	110	32	430	200	4200	6000	11	12	290	170
Elongate-Blocky Quartz 1	Vein_Quartz_23	14.2	4.9	820	300	117	37	250	250	7200	7300	5.6	8.2	70	120
	Vein_Quartz_24	0.33	0.29	81	21	24.5	2.7	28	18	480	540	bd	0.35	bd	15
	Vein_Quartz_25	15	12	690	290	120	110	610	400	70000	13000	49	55	110	210
	Vein_Quartz_26	bd	1.3	80	170	81	34	190	100	2100	4700	13	16	36	93
	Vein_Quartz_27	bd	4.3	550	230	151	41	400	330	6000	6400	bd	1.6	290	230
	Vein_Quartz_28	9.6	8.8	580	320	480	230	780	390	12000	11000	bd	17	420	680
	Vein_Quartz_29	7.9	7	550	320	740	770	450	230	bd	5600	8	20	bd	200
	Vein_Quartz_30	bd	5.3	150	240	107	57	210	220	bd	4700	bd	3	50	130
	Vein_Quartz_31	8.8	6.9	230	240	164	44	bd	190	5400	5600	bd	1	230	190
	Vein_Quartz_32	3.7	4.3	520	340	166	42	bd	210	5500	5600	1.4	2.7	270	180
	Vein_Quartz_33	2.3	1.1	55	25	38.1	5.2	bd	24	bd	680	1.25	0.84	22	23
	Vein_Quartz_34	0.69	0.41	20	24	24.5	5.6	bd	18	600	680	2.2	1.9	bd	16
	Vein_Quartz_35	1.6	5.4	330	200	206	56	bd	300	12000	7500	55	42	190	290
	Vein_Quartz_36	0.9	3.8	160	300	184	64	bd	220	2900	4400	bd	7.2	bd	190
	Vein_Quartz_37	7.3	7.4	300	260	187	66	bd	180	9600	6200	13	26	bd	170

	Vein_Quartz_38	bd	2.7	380	240	138	30	bd	220	5700	5000	bd	1.8	bd	160
	Vein_Quartz_39	2.4	4	310	310	137	41	100	210	5500	4000	bd	5.9	120	150
	Vein_Quartz_40	5.9	4	370	170	108	26	bd	140	6700	4300	bd	2.5	bd	100
	Vein_Quartz_41	7.9	3.1	330	180	77	33	bd	160	2300	5800	bd	2.3	bd	140
Fibrous Quartz 3	Vein_Quartz_42	2.6	3.4	590	240	130	42	bd	260	bd	6200	8	11	bd	200
	Vein_Quartz_43	12.7	6.6	400	190	146	36	bd	230	6300	8100	10	12	bd	150
	Vein_Quartz_44	bd	2.5	710	440	280	140	470	260	14100	8400	bd	1	bd	240
	Vein_Quartz_45	bd	0.16	42	12	17.8	2.8	15	11	520	380	0.67	0.52	7.4	9.8
	Vein_Quartz_46	2.8	3.7	510	250	122	22	180	230	11900	7600	2.3	4.1	50	170
	Vein_Quartz_47	0.44	0.22	38	16	11	1.9	bd	9.7	260	230	2.5	1.6	bd	8.6
	Vein_Quartz_48	7.2	4.1	620	370	173	59	80	170	12200	6500	30	39	bd	160
	Vein_Quartz_49	3.4	3	690	440	142	31	bd	180	10700	5400	bd	1.4	90	150
Subhedral Blocky Quartz 1	Vein_Quartz_50	10.3	5	840	300	178	43	130	170	12600	5500	8	11	250	210
	Vein_Quartz_51	6.2	4.3	610	270	152	41	bd	280	4900	6800	bd	1.8	160	210
	Vein_Quartz_52	1.18	0.73	134	51	39.3	8.1	59	39	bd	1100	2.4	2	42	32
	Vein_Quartz_53	13.5	9.1	480	180	191	42	bd	220	7200	6300	10	12	220	180
	Vein_Quartz_54	18	13	420	380	600	280	70	280	16700	9300	6.9	7.9	320	260
	Vein_Quartz_55	bd	0.049	7.6	4	10.3	3	bd	6.2	bd	98	0.79	0.28	bd	3.3
Elongate-Blocky Quartz 2	Vein_Quartz_56	27	16	1560	840	177	67	120	310	10500	7400	21	24	310	210
	Vein_Quartz_57	0.92	0.49	74	33	19.7	3.6	bd	20	890	320	0.58	0.56	bd	13
	Vein_Quartz_58	8	4.6	550	250	97	30	bd	200	2600	3300	3.6	7.2	80	130
	Vein_Quartz_59	12	12	1000	1200	299	97	bd	630	24000	15000	4.7	8.2	490	600
	Vein_Quartz_60	23	14	470	440	257	81	bd	330	14000	16000	bd	1	230	310
Subhedral Blocky Quartz 2	Vein_Quartz_61	17	16	510	450	260	120	bd	250	80000	11000	bd	0.1	170	240
	Vein_Quartz_62	8.8	8.6	750	370	480	500	540	330	11000	10000	4.2	9.9	4300	3100
	Vein_Quartz_63	11.2	7.6	690	300	510	220	190	310	100000	14000	1.9	6	710	440
	Vein_Quartz_64	8.2	1.2	75	25	67.6	5.5	bd	11	bd	380	0.64	0.69	bd	10
	Vein_Quartz_65	bd	4.4	470	320	270	73	170	240	15000	9700	35	32	200	190

	Sample Number														
Wallrock Quartz	Wallrock_1	9	12	550	390	246	74	bd	310	100000	11000	bd	1.9	230	260
	Wallrock_2	2.3	4.2	460	660	1310	560	760	730	100000	11000	bd	7.2	550	330
	Wallrock_3	6.4	6.5	410	350	310	110	bd	320	bd	6800	bd	14	310	310
	Wallrock_4	18	12	320	590	206	59	200	250	80000	10000	9	17	300	280
	Wallrock_5	13.2	6.4	bd	210	430	180	50	300	8600	6800	bd	12	190	240
	Wallrock_6	12	12	bd	250	500	200	100	260	6400	7200	6	18	220	300
	Wallrock_7	4.1	7.3	340	210	334	80	bd	250	10500	5900	bd	6.9	330	140
	Wallrock_8	bd	4.3	570	280	1180	450	830	590	11700	9400	38	35	730	360
	Wallrock_9	2.5	5.4	500	330	212	66	bd	280	13000	7100	bd	9.7	250	270
	Wallrock_10	12	11	1120	750	410	140	bd	640	90000	12000	35	42	150	650
	Wallrock_11	bd	3.6	520	330	640	230	bd	200	2100	5500	4	9.8	230	330
	Wallrock_12	13.7	9.9	290	300	440	190	bd	310	3300	6400	9	12	bd	240

	Sample Number	Ga69		Ge72		As75		Sr88		Sn118		Sb121		Ba137	
		(ppm)	2SE (ppm)	(ppm)	2SE (ppm)	(ppm)	2SE (ppm)	(ppm)	2SE (ppm)	(ppm)	2SE (ppm)	(ppm)	2SE (ppm)	(ppm)	2SE (ppm)
BCR Standard	BCR_Standard_1	134.2	1.8	3.79	0.41	1.11	0.54	611	10	6.16	0.33	0.7	0.11	1215	20
	BCR_Standard_2	129.9	2.1	4.1	0.35	2.42	0.48	609	10	6.69	0.36	0.71	0.11	1204	22
	BCR_Standard_3	125.6	1.6	4.1	0.45	1.37	0.59	604	10	7.23	0.28	0.673	0.096	1191	22
NIST Standard	G_NIST612_1	35.68	0.63	35.18	0.67	35.4	1	77.2	1.1	37.33	0.72	36.91	0.66	38.8	1
	G_NIST612_2	36.36	0.57	34.85	0.66	39.2	1.3	79.6	1.2	37.96	0.53	38.55	0.65	39.68	0.94
	G_NIST612_3	36.45	0.68	34.73	0.81	38.3	1.1	78.7	1.6	38.1	0.62	39.23	0.74	40.8	1.1
	G_NIST612_4	36.01	0.49	35.21	0.63	37.03	0.87	79.2	1.4	38.41	0.71	38.28	0.61	40.12	0.87
	G_NIST612_5	35.37	0.66	35.05	0.97	36.9	1.2	79.1	1.4	38.81	0.72	37.72	0.83	39.75	0.85
	G_NIST612_6	36.04	0.61	35.15	0.73	36.3	1.2	77.9	1.3	37.97	0.55	37.48	0.66	39.22	0.86
	G_NIST612_7	35.81	0.65	34.5	0.68	36.6	1.1	78.3	1.1	38.42	0.68	37.98	0.56	40.1	0.78
	G_NIST612_8	35.7	0.49	35.04	0.79	37.1	1	78	1.1	37.4	0.61	38.11	0.62	38.8	0.91

	G_NIST612_9	36.55	0.56	35.36	0.84	37.1	1.1	78.6	1.3	37.88	0.54	37.84	0.7	40.1	1
Fibrous Quartz 1	Vein_Quartz_1	48	57	210	210	590	530	1.01	0.91	80	140	21	36	30	15
	Vein_Quartz_2	bd	0.25	2.8	1.8	11.8	5.7	0.08	0.058	3	1	0.6	0.52	0.25	0.22
	Vein_Quartz_3	bd	5.7	9	37	168	87	0.018	0.037	11	21	3	9.3	1.4	2.7
	Vein_Quartz_4	20	20	bd	170	740	480	bd	1	bd	79	17	37	bd	1
	Vein_Quartz_5	bd	0.59	bd	3.7	15	10	0.112	0.095	2	2.4	4.3	1.4	bd	1
	Vein_Quartz_6	27	20	bd	66	240	160	8.2	9.4	bd	27	41	25	12	13
	Vein_Quartz_7	bd	6.6	40	89	bd	140	1	2.1	bd	22	7.3	9.5	3.7	5.2
	Vein_Quartz_8	1.7	1.2	bd	9	21	17	0.81	0.49	bd	3.8	7	4.3	5.8	4.8
	Vein_Quartz_9	19	22	bd	81	260	240	2	1.7	50	110	33	23	bd	1
	Vein_Quartz_10	7.5	9.8	bd	49	160	120	4.8	3.6	bd	27	29	17	7	10
	Vein_Quartz_11	bd	4.3	bd	33	41	78	2	1.7	9.4	7	4	10	1.6	1.9
Fibrous Quartz 2	Vein_Quartz_12	1	5.4	bd	32	bd	66	0.39	0.41	bd	17	7	11	0.1	0.2
	Vein_Quartz_13	bd	5.1	11	36	77	64	0.27	0.35	16	13	13	10	bd	1
	Vein_Quartz_14	1.6	4.2	bd	25	26	42	1	1.6	bd	8	1.7	7.1	0.23	0.3
	Vein_Quartz_15	bd	6.2	28	33	bd	64	2.6	2.5	bd	18	17	13	0.8	1.3
	Vein_Quartz_16	bd	5.7	bd	37	bd	83	0.016	0.024	bd	23	17	13	2.2	2.6
	Vein_Quartz_17	bd	6.2	bd	46	57	77	0.87	0.94	bd	23	19	13	0.11	0.22
	Vein_Quartz_18	bd	2	8	19	14	18	0.59	0.45	bd	5.3	5.9	6.8	bd	0.44
	Vein_Quartz_19	5.2	7.2	19	48	bd	77	0.4	0.59	36	28	2	13	bd	1
	Vein_Quartz_20	7.9	6.6	bd	31	bd	85	0.52	0.6	37	23	15	11	bd	0.43
	Vein_Quartz_21	bd	0.39	bd	3.1	bd	6.6	bd	1	4	2.3	0.74	0.72	bd	1
	Vein_Quartz_22	4.6	4.7	bd	28	29	46	0.18	0.36	12	16	7.5	8.9	bd	1
Elongate-Blocky Quartz 1	Vein_Quartz_23	6	5.2	bd	28	17	55	0.09	0.12	12	14	15	11	bd	1
	Vein_Quartz_24	bd	0.32	bd	2.3	bd	5.9	0.07	0.05	5.3	1.7	0.9	0.75	0.15	0.14
	Vein_Quartz_25	4.9	9.1	bd	49	90	120	0.47	0.53	17	33	17	15	bd	1
	Vein_Quartz_26	bd	2.1	bd	17	10	28	0.16	0.19	1.8	8.3	5.1	5.6	0.032	0.063
	Vein_Quartz_27	bd	7.9	bd	38	37	83	0.1	0.2	45	22	6.6	7.7	12	15

49

Group	Sample														
	Vein_Quartz_28	bd	7.6	bd	55	100	110	1.9	2.7	23	18	19	20	1.5	2
	Vein_Quartz_29	bd	4.4	16	42	bd	60	1.2	1.2	35	26	24	12	0.17	0.26
	Vein_Quartz_30	bd	2.7	bd	49	bd	72	0.1	0.1	4	13	bd	8	1.3	2.7
	Vein_Quartz_31	bd	5.4	32	31	51	61	bd	1	8	20	17.2	9.2	1.3	2.6
	Vein_Quartz_32	bd	3.8	19	31	bd	59	0.08	0.15	bd	16	15	9.6	bd	1
	Vein_Quartz_33	bd	0.54	bd	4.4	9.6	6.8	0.029	0.033	3.7	2.2	1.1	1.3	0.18	0.2
	Vein_Quartz_34	bd	0.4	bd	2.6	18.2	6.4	bd	1	5.6	1.9	bd	0.95	0.024	0.033
	Vein_Quartz_35	bd	6.9	bd	43	140	64	bd	1	29	25	10	11	bd	1
	Vein_Quartz_36	bd	5.2	bd	34	114	55	0.54	0.72	18	19	bd	8	bd	1
	Vein_Quartz_37	bd	5.9	bd	41	150	63	0.18	0.35	40	26	5.4	9.5	bd	1
	Vein_Quartz_38	bd	4.1	bd	38	119	57	0.42	0.42	30	16	14	10	0.3	0.6
	Vein_Quartz_39	bd	3.4	bd	32	290	100	0.14	0.28	31	20	bd	7.2	bd	1
	Vein_Quartz_40	3.7	3	9	24	174	59	0.033	0.045	24	14	8.1	6.1	0.17	0.28
	Vein_Quartz_41	bd	2.6	56	27	29	50	bd	0.034	24	13	13.8	6.5	1.3	1.8
Fibrous Quartz 3	Vein_Quartz_42	bd	3.5	38	28	bd	66	bd	0.19	31	22	12.1	8.7	bd	1
	Vein_Quartz_43	bd	3.9	bd	28	53	99	0.74	0.9	13	15	17	10	bd	1
	Vein_Quartz_44	bd	6.5	bd	43	bd	120	0.028	0.04	28	22	18	11	bd	1
	Vein_Quartz_45	bd	0.23	bd	1.5	bd	4.6	0.108	0.053	4.7	1.3	0.55	0.57	0.059	0.069
	Vein_Quartz_46	5.8	5.9	bd	45	bd	85	0.22	0.29	14	15	3.1	7.7	0.33	0.65
	Vein_Quartz_47	bd	0.14	bd	1.1	bd	2.7	0.25	0.13	4.48	0.78	bd	0.38	0.57	0.34
	Vein_Quartz_48	bd	3.8	bd	27	130	100	bd	1	9	16	bd	7	bd	1
	Vein_Quartz_49	4.4	4.6	bd	27	230	100	0.41	0.44	23	18	2.4	8.3	bd	1
Subhedral Blocky Quartz 1	Vein_Quartz_50	bd	3.7	bd	24	210	99	0.018	0.026	37	19	bd	8.8	0.01	0.02
	Vein_Quartz_51	3.1	4.1	bd	30	60	92	0.056	0.08	24	19	bd	9	0.12	0.24
	Vein_Quartz_52	bd	0.8	bd	5.4	bd	16	0.043	0.05	4.9	3.6	bd	1.9	0.78	0.89
	Vein_Quartz_53	1	4.5	bd	35	bd	90	0.23	0.36	9	17	bd	7.2	1.5	2.3
	Vein_Quartz_54	4.7	8	bd	45	bd	150	1.1	1	39	34	8	11	bd	1
	Vein_Quartz_55	bd	0.061	1.3	0.7	bd	2.3	0.031	0.014	3.23	0.71	bd	0.1	0.076	0.051

	Sample													
Elongate-Blocky Quartz 2	Vein_Quartz_56	bd	3.9	bd	46	bd	140	1	1	30	20	9	11	0.13	0.26
	Vein_Quartz_57	bd	0.32	bd	3	bd	10	0.036	0.038	9.7	2.5	bd	0.69	0.01	0.02
	Vein_Quartz_58	3.5	3.9	bd	30	bd	100	bd	1	20	12	19.3	8.3	bd	1
	Vein_Quartz_59	17	29	bd	80	bd	200	0.17	0.29	14	33	48	21	bd	1
	Vein_Quartz_60	bd	7	bd	79	290	210	0.4	0.8	bd	30	8	16	bd	1
Subhedral Blocky Quartz 2	Vein_Quartz_61	bd	7.1	62	53	bd	160	0.34	0.68	bd	26	24	12	bd	1
	Vein_Quartz_62	5.8	7.5	bd	28	90	120	4.6	3.3	9	14	21	11	0.54	0.67
	Vein_Quartz_63	1.3	4.3	22	37	220	130	8.5	9.2	15	17	7	10	11	13
	Vein_Quartz_64	bd	0.22	2.7	1.7	bd	4.9	0.071	0.055	15.8	2.6	4.35	0.99	0.028	0.057
	Vein_Quartz_65	bd	5.7	13	36	bd	97	31	46	47	24	11	10	2.8	3.1
Wallrock Quartz	Wallrock_1	1.7	5.2	23	53	bd	130	0.49	0.53	28	26	20	18	0.02	0.04
	Wallrock_2	4.3	5	15	30	bd	84	0.81	0.64	30	19	19	12	6.5	6.3
	Wallrock_3	1.6	4.3	46	48	bd	97	3.2	2.1	19	43	9	10	0.07	0.14
	Wallrock_4	1.5	5.3	44	41	bd	86	0.051	0.061	22	20	24	13	2	2.8
	Wallrock_5	bd	4.4	49	42	bd	81	3	2	31	21	24	11	bd	1
	Wallrock_6	5.3	6	43	49	32	73	3.7	2.1	40	21	bd	13	2.8	2.4
	Wallrock_7	bd	4.3	95	39	bd	72	6.3	2.9	50	25	bd	7.6	4.6	5
	Wallrock_8	bd	4.7	41	37	bd	91	7.5	3.7	35	22	bd	12	42	23
	Wallrock_9	bd	4	71	49	bd	93	4.4	3	28	22	bd	12	13	11
	Wallrock_10	bd	6.6	72	52	bd	88	1.4	1.6	70	54	5	24	bd	1
	Wallrock_11	1.4	5.8	41	29	bd	130	0.39	0.37	18	14	3.4	8.8	6.8	9.5
	Wallrock_12	1	5.6	77	47	bd	81	2.1	1.8	10	22	16	13	22	20

Table 4: *Sample 'SH3_Thin'. 'bd' = below detection limits.*

	Sample Number	Li7		Na23		Al27		K39		Ca43		Ti47		Fe57	
		(ppm)	2SE (ppm)	(ppm)	2SE (ppm)	(ppm)	2SE (ppm)	(ppm)	2SE (ppm)	(ppm)	2SE (ppm)	(ppm)	2SE (ppm)	(ppm)	2SE (ppm)
BCR Standard	BCR_Standard_1	9.38	0.33	24380	160	74630	610	17560	130	48260	900	13520	130	40160	310
	BCR_Standard_2	9.27	0.34	24280	170	75530	640	17470	100	46940	630	13470	120	43600	360
	BCR_Standard_3	9.43	0.24	24420	150	76550	650	17630	130	48740	840	13860	120	49460	360
NIST Standard	G_NIST612_1	41.58	0.52	103070	880	11180	130	66.4	1.1	84900	1100	44.2	1.2	53.6	2.2
	G_NIST612_2	42.11	0.53	104200	1200	11270	110	66.6	1.1	86000	1300	43.6	1.4	51.7	2
	G_NIST612_3	42.77	0.57	104770	950	11200	110	66.39	0.93	85100	1200	44.4	1.3	52	1.7
	G_NIST612_4	41.94	0.6	103300	1100	10950	140	65.9	1.1	84400	1100	43.5	1.4	49.9	2
	G_NIST612_5	41.9	0.61	104200	1300	11120	130	66.6	1.1	84900	1500	44.7	1.3	50.8	1.9
	G_NIST612_6	41.64	0.58	104600	1100	11210	140	66	1	85200	1200	44.3	1.2	47.8	1.6
	G_NIST612_7	42.14	0.57	103200	1300	11120	130	65.96	0.95	84200	1400	43.7	1.7	50.7	1.8
	G_NIST612_8	42.08	0.84	104100	1900	11030	200	65.5	1.3	84600	1700	43	1.7	51.1	1.8
	G_NIST612_9	41.37	0.98	103300	2100	10850	260	66.2	1.2	84200	1800	42.5	1.4	49.5	2.4
	G_NIST612_10	42.13	0.6	105800	1700	11340	180	67.9	1.4	86100	1900	44.1	1.5	51.6	2.3
	G_NIST612_11	42.43	0.71	104800	1700	11230	140	66.4	1.1	85800	1300	44.8	1.6	52.8	2
	G_NIST612_12	41.55	0.76	102500	1100	11200	140	66	1.3	84600	1600	44.8	1.5	52.3	2.5
Blocky Quartz 1	Vein_Quartz_1	bd	0.9	300	77	50	13	bd	65	bd	1600	3	3.5	25	51
	Vein_Quartz_2	bd	0.56	156	32	43.5	6	bd	34	490	890	bd	1.2	17	23
	Vein_Quartz_3	0.39	0.36	183	63	40.6	4.9	17	28	1280	730	3.8	2.9	18	15
	Vein_Quartz_4	0.9	0.99	181	47	36.8	5.3	bd	26	960	880	7.6	4.1	bd	19
	Vein_Quartz_5	0.61	0.12	19.2	6.7	32.3	1.9	bd	4.3	165	94	1.62	0.46	9	13
	Vein_Quartz_6	7.2	5	800	230	200	41	170	180	5900	4200	bd	3.3	19	85
	Vein_Quartz_7	bd	3.3	660	170	194	38	180	170	4600	4800	bd	5.6	190	170
	Vein_Quartz_8	1	3.2	670	300	128	32	bd	180	4400	4500	bd	9.9	77	87
	Vein_Quartz_9	3.7	6	880	340	169	68	bd	350	6900	6000	bd	18	260	210
	Vein_Quartz_10	5	21	1260	800	220	210	160	700	90000	26000	bd	59	bd	340

	Sample													
	Vein_Quartz_11	19	20	790	330	360	160	bd	400	17000	12000	bd	9.5	180	210
	Vein_Quartz_12	4.9	4.8	840	270	184	53	bd	200	11800	5800	bd	5.8	90	130
	Vein_Quartz_13	bd	3.6	690	260	151	39	60	220	6700	7200	bd	12	60	130
	Vein_Quartz_14	bd	4.1	800	280	240	83	bd	190	6100	5600	4	17	160	310
	Vein_Quartz_15	20	17	570	320	296	76	570	450	12100	8100	18	25	bd	280
	Vein_Quartz_16	3	17	2400	3600	30	390	200	1100	bd	95000	bd	38	120	700
	Vein_Quartz_17	1.87	0.93	196	66	67	11	59	50	2700	1700	bd	3	bd	28
	Vein_Quartz_18	0.26	0.17	46	14	25	3.1	bd	9	bd	260	1.4	0.97	bd	6.9
	Vein_Quartz_19	0.97	0.61	47	17	19.2	2.7	13	11	bd	320	1.39	0.89	bd	7
	Vein_Quartz_20	7.1	4.7	1320	460	320	130	360	170	2600	5400	46	35	190	160
	Vein_Quartz_21	0.3	0.19	60	15	34.2	3	14	12	560	350	2	1.3	5	10
	Vein_Quartz_22	0.39	0.21	70	18	21.6	2.2	bd	11	600	370	bd	0.46	bd	7
Fibrous Quartz	Vein_Quartz_23	bd	0.12	253	88	52	16	32	16	bd	210	3.2	1.6	14.3	7.9
	Vein_Quartz_24	bd	3.7	540	200	257	58	30	280	20000	10000	bd	8.2	60	150
	Vein_Quartz_25	1.57	0.15	32.6	5	37.5	2.1	6.3	1.9	101	54	2.88	0.84	bd	1.2
	Vein_Quartz_26	bd	8.1	1900	1300	410	210	450	650	39000	29000	7	21	1000	1300
	Vein_Quartz_27	bd	0.036	11.7	2.7	13.3	1.8	3.7	3.9	bd	57	2.21	0.99	bd	1
	Vein_Quartz_28	0.07	0.045	25.8	5.8	11.63	0.75	bd	1.7	bd	36	1.53	0.46	bd	1.1
	Vein_Quartz_29	0.063	0.025	10.9	2.3	10.3	1.8	bd	0.88	bd	27	1.56	0.34	2.1	1.4
	Vein_Quartz_30	0.119	0.089	28.5	8	10.9	1	bd	3	bd	110	1.4	0.68	bd	2.3
	Vein_Quartz_31	0.073	0.035	28.9	9.9	10.8	1.2	2.6	1.3	bd	39	1.59	0.42	bd	1.2
	Vein_Quartz_32	bd	0.035	21.5	4.7	7.9	1.6	5.9	3.5	bd	76	1.67	0.62	bd	1.6
	Vein_Quartz_33	12.3	9.6	2120	860	240	110	750	700	13000	12000	9	18	190	440
	Vein_Quartz_34	0.9	5.2	1010	700	480	120	370	440	7200	7000	bd	1.1	170	230
	Vein_Quartz_35	2.9	7	1040	610	372	98	510	230	bd	5500	4.4	5	210	190
	Vein_Quartz_36	bd	0.11	58	32	41	22	23	23	bd	97	1.9	1.2	12.7	7.1
	Vein_Quartz_37	bd	0.32	83	35	22.8	5.2	23	16	bd	270	1.29	0.81	bd	6.5
	Vein_Quartz_38	bd	3.6	1440	600	330	130	350	290	bd	5500	bd	1	bd	160
	Vein_Quartz_39	bd	3	3100	1300	340	160	280	250	bd	4500	29	38	bd	170

	Sample													
	Vein_Quartz_40	1.7	1.7	236	35	69	20	bd	67	bd	1900	8.6	6.7	bd	33
	Vein_Quartz_41	1.54	0.23	10.3	3	28.8	1.2	2	1.5	78	35	2.3	0.45	bd	0.48
	Vein_Quartz_42	3	4.8	2500	1800	290	180	570	490	bd	8500	7	19	170	160
	Vein_Quartz_43	0.93	0.098	64	88	37.4	8.1	9	11	80	100	3.51	0.63	bd	1.2
Blocky Quartz 2	Vein_Quartz_44	4.2	4.4	1120	370	202	60	110	360	9900	5500	bd	8.9	130	180
	Vein_Quartz_45	6.5	7.5	1810	830	340	110	270	390	bd	7400	bd	1.2	160	260
	Vein_Quartz_46	3.1	5	910	390	320	190	bd	530	60000	14000	33	64	bd	210
	Vein_Quartz_47	1.35	0.85	111	35	32.4	2.8	bd	17	520	510	0.6	1	bd	17
	Vein_Quartz_48	6.3	6	1190	410	290	110	bd	320	bd	7800	bd	1.5	50	130
	Vein_Quartz_49	8.7	4.1	890	350	176	82	bd	210	2400	5000	12	17	bd	180
	Vein_Quartz_50	0.7	0.53	169	51	41.4	8.9	bd	26	600	490	bd	0.012	bd	19
	Vein_Quartz_51	bd	0.18	68	14	18.9	5	bd	11	1050	660	1.3	1.5	29	13
	Vein_Quartz_52	2	3.9	670	270	205	82	350	230	12100	9300	20	25	70	170
	Vein_Quartz_53	4.2	3.6	1040	360	266	57	380	200	bd	3600	11	16	118	85
	Vein_Quartz_54	4	5.9	3500	2400	270	190	240	260	5800	6900	16	26	150	220
	Vein_Quartz_55	9.6	8	670	400	146	67	bd	290	2600	5400	bd	1	bd	170
	Vein_Quartz_56	4.2	5.4	1900	1200	270	90	350	430	12500	8500	10	20	bd	220
	Vein_Quartz_57	2.9	5.3	3800	3400	440	190	1010	690	4000	6500	11	15	440	340
	Vein_Quartz_58	9.2	8.6	1740	600	210	75	bd	470	1900	6500	bd	1	190	350
	Vein_Quartz_59	5.3	5.5	1070	450	136	52	bd	200	9900	7500	8	11	bd	140
	Vein_Quartz_60	24	18	1200	510	240	61	bd	280	100000	13000	bd	1	260	260
	Vein_Quartz_61	bd	2.5	950	300	197	88	bd	150	7600	5200	7	8.5	370	250
	Vein_Quartz_62	6.9	6.7	760	440	380	180	140	260	13300	8300	bd	1	bd	260
	Vein_Quartz_63	3.7	4.9	890	320	113	32	bd	190	4500	4300	1.3	2.1	180	130
	Vein_Quartz_64	4.9	4.1	800	230	178	40	130	130	3700	4600	bd	1	130	120
	Vein_Quartz_65	1.1	5.5	560	410	153	50	bd	260	11200	6400	18	32	40	290
	Vein_Quartz_66	2.1	4	1100	460	188	50	30	230	6100	6800	8.5	8.6	210	190
	Vein_Quartz_67	2.1	5.7	570	290	280	120	210	210	7800	7200	3.8	7.6	80	130
	Vein_Quartz_68	2.6	5.6	630	400	194	47	140	230	9970	7800	21	18	80	130

	Vein_Quartz_69	2.2	4.9	940	270	186	59	140	240	5900	5400	6	7.2	bd	180
	Vein_Quartz_70	bd	6.4	330	380	187	54	110	270	15000	12000	0.025	0.051	bd	130
	Vein_Quartz_71	0.24	0.14	163	47	13.9	3	10.9	5.8	380	290	2.7	1.3	9	7.5
	Vein_Quartz_72	0.47	0.43	153	31	20.4	3.8	44	19	950	510	1.7	1.2	bd	18
	Vein_Quartz_73	5.8	4.6	840	360	166	39	280	150	bd	4200	3.4	6.6	bd	130
	Vein_Quartz_74	4.6	5.6	360	250	236	76	220	230	4900	6500	4.2	6.1	bd	220
	Vein_Quartz_75	1.3	3.9	520	220	219	69	180	220	16000	11000	0.69	0.94	170	200
	Vein_Quartz_76	3.6	6.7	130	270	316	65	bd	310	12000	12000	4.9	9.9	bd	300
	Vein_Quartz_77	1	2.9	210	180	147	38	260	190	6300	6600	11	15	bd	180
	Vein_Quartz_78	3	4.4	1550	990	370	110	340	420	40000	17000	18	25	bd	300
	Vein_Quartz_79	0.37	0.39	410	270	80	33	106	36	bd	520	3.4	3.7	26	27
	Vein_Quartz_80	0.7	3.3	930	390	322	90	220	330	17000	14000	20	28	bd	250
	Vein_Quartz_81	5	4	620	270	269	64	320	190	9000	5500	10	11	bd	170
	Vein_Quartz_82	3.1	6.1	340	350	300	160	190	420	12000	10000	61	62	bd	280
Border Quartz	Vein_Quartz_83	6.2	4.3	630	200	293	50	340	310	6500	6300	bd	1	bd	210
	Vein_Quartz_84	5.4	3.2	550	210	250	150	120	210	1500	5800	0.45	0.64	90	130
	Vein_Quartz_85	11	7.7	250	220	286	90	140	200	bd	5600	0.22	0.43	40	180
	Vein_Quartz_86	0.54	0.68	134	36	257	51	157	35	bd	1500	4	3.9	41	38
	Vein_Quartz_87	3	1.6	126	71	114	23	39	82	bd	3300	bd	1	bd	71
	Vein_Quartz_88	4	3.9	bd	200	208	63	bd	200	1500	6900	23	26	40	180
	Vein_Quartz_89	13.3	9.3	130	200	410	140	190	300	bd	6100	8	16	200	380
	Vein_Quartz_90	4.3	3.1	350	250	196	58	60	200	7800	7200	16	19	220	180
	Vein_Quartz_91	7.4	5.1	120	220	223	74	bd	290	60000	11000	bd	0.57	bd	160
Wallrock Quartz	Wallrock_1	3.3	8.3	460	260	1190	750	540	410	13900	7300	bd	14	bd	300
	Wallrock_2	37	24	610	270	12100	3500	8500	2100	8100	5600	25	43	700	260
	Wallrock_3	9.4	6.7	320	200	660	190	540	240	21000	8100	bd	27	bd	490
	Wallrock_4	14	6.1	357	77	1620	440	460	140	940	930	4.7	9.1	800	1200
	Wallrock_5	147	36	620	260	36400	6400	660	350	10200	7200	18	28	15900	4100
	Wallrock_6	16.5	8.9	690	450	4800	3600	230	320	bd	2200	120	140	4200	3300

	Ga69		Ge72		As75		Sr88		Sn118		Sb121		Ba137	
Wallrock_7	32	14	610	200	4700	1300	bd	370	9500	7600	bd	9.9	2500	1000
Wallrock_8	67.1	6.2	61.5	4.3	35700	2900	223	13	bd	72	67.9	6.6	21300	1500
Wallrock_9	1.4	7	1310	380	890	330	bd	400	80000	10000	bd	0.66	440	380
Wallrock_10	bd	1.9	590	160	192	76	bd	150	bd	3600	5.3	7.4	bd	91
Wallrock_11	bd	4.7	1250	390	940	340	130	160	4800	4800	5.8	6.4	610	430

	Sample Number	Ga69		Ge72		As75		Sr88		Sn118		Sb121		Ba137	
		(ppm)	2SE (ppm)	(ppm)	2SE (ppm)	(ppm)	2SE (ppm)	(ppm)	2SE (ppm)	(ppm)	2SE (ppm)	(ppm)	2SE (ppm)	(ppm)	2SE (ppm)
BCR Standard	BCR_Standard_1	71.4	1.1	1.99	0.27	0.72	0.38	316	3.8	3.06	0.21	0.495	0.087	636.1	9.8
	BCR_Standard_2	70.15	0.93	1.78	0.28	0.58	0.65	311.6	3.3	2.95	0.23	0.391	0.082	634.6	7.6
	BCR_Standard_3	70.54	0.87	2.14	0.28	0.85	0.36	315	3.4	3.32	0.26	0.367	0.072	644.6	8.9
NIST Standard	G_NIST612_1	36.47	0.4	35.22	0.68	35.9	1.2	78.2	1.2	38.18	0.54	37.17	0.59	39.71	0.82
	G_NIST612_2	35.69	0.47	35.4	0.57	35	1.1	79.2	1.1	37.74	0.56	37.66	0.55	40.49	0.64
	G_NIST612_3	36.16	0.46	35.53	0.61	38.79	0.99	79.1	1	38.75	0.61	38.71	0.45	39.63	0.82
	G_NIST612_4	35.66	0.51	34.64	0.7	37.14	0.91	77.2	1.2	38.14	0.48	37.91	0.56	38.89	0.69
	G_NIST612_5	35.99	0.54	34.08	0.63	37.5	1.1	78.46	0.99	37.8	0.57	38.47	0.51	39.75	0.81
	G_NIST612_6	35.76	0.39	34.24	0.64	37.35	0.91	78.1	1.1	37.9	0.58	37.89	0.48	39.94	0.81
	G_NIST612_7	35.82	0.55	34.69	0.81	37.02	0.86	78.24	0.93	37.08	0.63	38.19	0.63	39.15	0.7
	G_NIST612_8	35.54	0.66	35.31	0.81	37.3	1	76.7	1.4	37.92	0.86	38.07	0.8	39.05	0.98
	G_NIST612_9	35.4	0.8	35.23	0.82	37.2	1.2	77.7	1.7	36.29	0.89	37.08	0.86	38.8	1.1
	G_NIST612_10	36.88	0.6	35.57	0.99	37.6	1.4	79.6	1.2	38.27	0.95	38.62	0.83	40.36	0.88
	G_NIST612_11	35.99	0.63	35.16	0.96	36	1.1	79.2	1.2	38.57	0.74	38.07	0.64	40.5	1
	G_NIST612_12	36.24	0.52	35.27	0.65	36.4	1.1	78.1	1.3	38.54	0.55	37.43	0.63	40.2	1.1
Blocky Quartz 1	Vein_Quartz_1	1.2	1.2	bd	8.9	bd	17	bd	1	bd	5.8	2.2	2.7	bd	1
	Vein_Quartz_2	bd	0.63	bd	4.1	11	8.5	0.048	0.041	3	2.5	1.7	1.4	bd	1
	Vein_Quartz_3	bd	0.61	4	5	22.5	9.9	0.038	0.046	3	2.6	bd	1.3	bd	1
	Vein_Quartz_4	bd	0.38	bd	4.1	21	12	0.124	0.098	bd	2.1	bd	1.4	0.038	0.075

	Vein_Quartz_5	0.121	0.07	2.01	0.64	5	2.3	0.0257	0.0098	1.37	0.3	bd	0.19	0.0049	0.007
	Vein_Quartz_6	bd	2.5	9	21	39	51	0.11	0.12	16	14	bd	6.3	0.18	0.22
	Vein_Quartz_7	bd	3	bd	27	bd	53	0.033	0.051	25	14	bd	8.4	0.13	0.22
	Vein_Quartz_8	bd	2.7	bd	22	217	89	0.038	0.055	bd	16	1.4	8.3	bd	1
	Vein_Quartz_9	bd	5.8	6	48	350	210	0.013	0.016	35	47	7	13	bd	1
	Vein_Quartz_10	bd	11	bd	170	180	130	0.0035	0.007	66	59	16	47	0.23	0.3
	Vein_Quartz_11	bd	6.5	bd	46	bd	120	1.7	2.4	20	34	5	16	bd	1
	Vein_Quartz_12	1.7	4.2	bd	24	bd	61	0.22	0.32	12	17	20	13	bd	1
	Vein_Quartz_13	3.5	5.6	bd	37	bd	57	0.028	0.039	bd	21	9.3	7.2	bd	1
	Vein_Quartz_14	1.3	6	bd	29	193	74	0.117	0.096	bd	25	6.7	9.8	bd	1
	Vein_Quartz_15	2	6.2	bd	40	bd	120	0.06	0.071	18	29	18	12	0.35	0.65
	Vein_Quartz_16	16	19	bd	50	bd	710	0.38	0.46	12	30	bd	47	0.09	0.12
	Vein_Quartz_17	bd	0.74	bd	7.1	32	18	bd	1	7.5	4.2	bd	2	bd	1
	Vein_Quartz_18	bd	0.21	bd	2.3	13.8	4.8	0.017	0.02	3.8	1.2	bd	0.44	bd	1
	Vein_Quartz_19	bd	0.23	bd	1.2	11.1	5.8	0.015	0.014	4	1.2	bd	0.39	bd	1
	Vein_Quartz_20	bd	3.5	bd	37	270	130	0.35	0.49	27	23	17	12	bd	1
	Vein_Quartz_21	bd	0.2	bd	1.9	bd	4	0.069	0.085	1.8	1.3	0.74	0.63	0.009	0.017
	Vein_Quartz_22	bd	0.22	bd	1.5	bd	4.3	0.098	0.055	2.5	1.3	0.52	0.65	1.19	0.78
Fibrous Quartz	Vein_Quartz_23	bd	0.18	bd	1.9	bd	2.3	0.17	0.13	1.6	1.3	bd	0.46	0.07	0.14
	Vein_Quartz_24	4	5.6	15	50	200	150	bd	1	7	46	8.1	7.4	bd	1
	Vein_Quartz_25	0.094	0.043	1.54	0.27	2.6	1.1	0.101	0.031	0.85	0.15	0.22	0.11	0.27	0.13
	Vein_Quartz_26	bd	16	bd	94	490	240	17	17	bd	62	20	30	1.6	3.2
	Vein_Quartz_27	bd	0.045	1.33	0.42	2.27	0.99	bd	1	1.21	0.24	bd	0.12	0.13	0.11
	Vein_Quartz_28	bd	0.045	1.24	0.23	4.6	1.3	0.028	0.018	1.04	0.3	bd	0.1	0.054	0.051
	Vein_Quartz_29	0.066	0.028	1.3	0.19	2.53	0.8	0.09	0.023	1.17	0.13	bd	0.046	0.038	0.031
	Vein_Quartz_30	0.223	0.085	1.73	0.54	2.5	1.9	0.07	0.034	1.26	0.52	bd	0.16	0.11	0.12
	Vein_Quartz_31	bd	0.032	1.28	0.37	bd	0.78	0.0137	0.0083	0.89	0.21	0.118	0.071	0.05	0.053
	Vein_Quartz_32	0.099	0.077	1.22	0.52	bd	1.1	0.0032	0.0048	1.54	0.45	bd	0.1	bd	1
	Vein_Quartz_33	bd	7.9	17	42	480	220	0.65	0.89	bd	42	bd	15	bd	1

	Vein_Quartz_34	bd	3.3	bd	25	400	280	0.81	0.8	5	21	6.1	9.9	1.9	3.4
	Vein_Quartz_35	bd	3.3	bd	27	330	170	0.16	0.19	bd	8.6	6	13	0.3	0.61
	Vein_Quartz_36	bd	0.061	2.23	0.97	3.5	3.2	0.068	0.08	1.22	0.61	0.26	0.17	0.15	0.16
	Vein_Quartz_37	bd	0.12	bd	0.87	8.9	5.7	bd	1	1.8	0.91	bd	0.4	bd	0.19
	Vein_Quartz_38	bd	4.5	bd	14	210	120	bd	1	bd	12	bd	7.8	bd	1
	Vein_Quartz_39	bd	3.4	bd	53	310	290	0.34	0.53	bd	27	9	12	1.6	3.2
	Vein_Quartz_40	bd	1.2	bd	4.4	bd	7.5	0.44	0.46	bd	5.4	2.1	2.8	bd	1
	Vein_Quartz_41	0.058	0.031	1.65	0.33	bd	0.81	0.0155	0.0092	0.96	0.14	0.124	0.072	0.027	0.031
	Vein_Quartz_42	bd	4.8	bd	56	620	570	4	3.4	bd	22	12	12	3.7	6
	Vein_Quartz_43	0.076	0.047	2.02	0.21	4.1	2	0.09	0.1	1.15	0.27	0.183	0.083	0.15	0.19
Blocky Quartz 2	Vein_Quartz_44	bd	4	bd	33	50	120	1.3	1.3	bd	15	bd	12	bd	1
	Vein_Quartz_45	bd	5.4	bd	33	220	180	1.6	1.5	38	34	3	14	3.7	5.8
	Vein_Quartz_46	3	13	46	34	430	310	bd	1	19	24	18	21	bd	1
	Vein_Quartz_47	bd	0.34	bd	2.3	33	14	0.041	0.057	2.6	1.3	bd	0.53	bd	1
	Vein_Quartz_48	bd	4.3	bd	32	300	180	0.043	0.085	22	32	29	19	bd	1
	Vein_Quartz_49	bd	5.4	bd	36	410	180	0.39	0.75	17	16	8.9	6.5	0.07	0.13
	Vein_Quartz_50	bd	0.57	bd	3.2	bd	14	0.16	0.15	3	3.1	1	1	0.09	0.18
	Vein_Quartz_51	0.36	0.37	bd	3	bd	10	0.1	0.11	3.6	1.8	bd	0.67	bd	1
	Vein_Quartz_52	2	4.1	21	25	240	170	bd	1	13	17	4	13	bd	0.17
	Vein_Quartz_53	1.9	3.4	bd	20	400	220	0.26	0.25	33	27	11	12	2.7	5.2
	Vein_Quartz_54	bd	5.2	18	25	250	170	0.35	0.48	bd	13	5	11	bd	1
	Vein_Quartz_55	2.5	4.3	bd	20	690	270	0.11	0.15	11	35	5.6	9.5	bd	1
	Vein_Quartz_56	7.1	7.8	bd	33	680	250	1.4	2	bd	28	3.7	9.5	bd	1
	Vein_Quartz_57	bd	3.7	bd	35	530	350	4.1	6.1	16	17	bd	8.8	49	79
	Vein_Quartz_58	5.7	6.7	11	35	1020	380	0.13	0.19	21	28	bd	13	bd	1
	Vein_Quartz_59	bd	4.6	bd	27	290	180	0.44	0.63	21	25	bd	10	0.37	0.49
	Vein_Quartz_60	4	7	bd	46	460	270	bd	1	bd	30	7	14	bd	1
	Vein_Quartz_61	bd	3	5	31	bd	140	0.078	0.093	bd	20	bd	8.3	bd	1
	Vein_Quartz_62	bd	2.6	10	38	400	230	0.07	0.13	bd	18	11	12	bd	1

	Sample													
	Vein_Quartz_63	bd	3.5	bd	29	240	120	0.39	0.58	7	17	bd	8.1	bd	1
	Vein_Quartz_64	bd	2.3	bd	16	90	93	0.36	0.43	bd	13	10	9.1	bd	1
	Vein_Quartz_65	bd	5.6	bd	35	240	170	bd	1	12	29	15	16	bd	1
	Vein_Quartz_66	bd	4.2	bd	27	230	160	0.2	0.21	bd	13	bd	6.5	0.31	0.51
	Vein_Quartz_67	1.1	4.1	bd	33	370	160	0.006	0.013	25	24	5	11	bd	1
	Vein_Quartz_68	2.2	5.3	bd	32	290	180	0.47	0.56	16	18	6	11	bd	1
	Vein_Quartz_69	5.1	6.5	bd	36	390	210	0.27	0.31	9	26	2.4	9.9	bd	1
	Vein_Quartz_70	bd	4.8	bd	35	500	380	0.32	0.4	30	40	11	13	bd	1
	Vein_Quartz_71	bd	0.15	bd	0.92	5.4	6.3	0.077	0.04	4.2	1.2	0.35	0.33	0.0044	0.0089
	Vein_Quartz_72	bd	0.39	bd	2.3	14	12	0.018	0.02	2.8	1.6	1.05	0.54	0.056	0.063
	Vein_Quartz_73	1.3	3.7	bd	21	143	98	0.2	0.23	11	12	11.6	6.4	bd	1
	Vein_Quartz_74	bd	3.9	bd	30	60	140	1.5	1.3	13	26	3.3	8.7	bd	1
	Vein_Quartz_75	bd	3.8	bd	27	bd	100	0.086	0.093	24	27	9	12	0.66	0.96
	Vein_Quartz_76	3.3	9.2	20	50	bd	200	3.2	2.8	35	40	bd	15	bd	1
	Vein_Quartz_77	4.6	4.8	bd	31	20	120	1.2	1.5	35	23	bd	11	bd	1
	Vein_Quartz_78	6	6.1	bd	54	130	160	0.17	0.19	100	110	12	23	bd	1
	Vein_Quartz_79	bd	0.31	4.8	9.2	30	25	0.4	0.37	bd	1.8	bd	0.76	0.037	0.074
	Vein_Quartz_80	3.5	6.2	bd	40	130	160	0.8	1.1	39	29	8	15	bd	1
	Vein_Quartz_81	4.2	4.2	bd	29	bd	98	1.2	1.1	22	22	8.8	9.6	0.053	0.088
	Vein_Quartz_82	3.2	5	15	49	bd	130	bd	1	22	42	bd	12	bd	1
Border Quartz	Vein_Quartz_83	10.9	7.5	bd	35	50	120	0.35	0.59	21	21	bd	9.6	bd	1
	Vein_Quartz_84	4.8	4.9	bd	28	11	60	0.044	0.047	14	20	11.7	9.3	0.24	0.34
	Vein_Quartz_85	1.7	4	bd	35	90	110	0.044	0.062	bd	11	bd	6.9	0.036	0.073
	Vein_Quartz_86	1.9	1.1	bd	8.4	bd	21	0.35	0.39	8.4	3.7	2.3	2.1	bd	1
	Vein_Quartz_87	bd	1.5	bd	15	21	53	0.17	0.24	14	10	bd	4.2	bd	1
	Vein_Quartz_88	bd	3.3	bd	26	80	120	0.31	0.62	15	19	7	12	0.07	0.14
	Vein_Quartz_89	bd	4.1	bd	28	bd	94	2.8	2.2	bd	23	5.2	9.5	bd	1
	Vein_Quartz_90	3.1	3.1	bd	27	100	120	0.75	0.67	bd	17	12	10	bd	1
	Vein_Quartz_91	5.2	5.3	bd	44	60	150	0.62	0.71	21	34	19	15	0.046	0.093

Wallrock Quartz	Wallrock_1	bd	5.3	33	59	23	79	20.6	6.9	bd	30	34	17	2	2.9
	Wallrock_2	13	10	5	27	81	50	9.9	4.4	15	15	11.7	7.9	54	27
	Wallrock_3	bd	3.8	bd	33	23	48	14.2	5.9	bd	21	28	11	9.4	7.2
	Wallrock_4	2.4	2.6	bd	8.3	bd	12	2.8	1.2	4.9	6.1	6.8	2.3	8.2	4.5
	Wallrock_5	4.5	3.9	bd	32	150	130	3.7	1.7	bd	22	18.5	8.8	11	7.5
	Wallrock_6	7.3	6.3	bd	9.6	24	24	4	2.4	bd	6	3	2.7	1.9	2.7
	Wallrock_7	4.7	4.7	bd	30	225	99	2.9	1.6	bd	18	28	14	0.5	0.79
	Wallrock_8	4.53	0.35	bd	0.27	105	22	1.5	0.2	0.99	0.27	3.23	0.26	1	0.22
	Wallrock_9	8.1	6.3	bd	31	330	130	20	30	bd	30	32	14	0.53	0.9
	Wallrock_10	bd	2.1	bd	12	bd	39	0.2	0.28	bd	9.5	12	7.3	bd	1
	Wallrock_11	bd	3.4	bd	32	bd	66	1.7	1.3	bd	22	8	10	2.5	3.8

Table 5: Sample 'NG4_Thin'. 'bd' = below detection limits.

	Spot Label	Li7		Na23		Al27		K39		Ca43		Ti47		Fe57	
		(ppm)	2SE (ppm)	(ppm)	2SE (ppm)	(ppm)	2SE (ppm)	(ppm)	2SE (ppm)	(ppm)	2SE (ppm)	(ppm)	2SE (ppm)	(ppm)	2SE (ppm)
Standards	G_NIST612_1	41.8	0.54	104120	880	11221	86	70.3	5.4	85200	940	43.6	1.2	50.5	2
	G_NIST612_2	42.39	0.51	103960	860	11104	92	71.8	5.7	84700	1000	44.1	1.2	52.5	1.8
	G_NIST612_3	41.91	0.52	102800	1100	11170	110	64.9	2.1	85400	1200	45.4	1.4	49.7	2.1
	G_NIST612_4	41.97	0.4	103800	1100	11130	78	65	1.9	84580	870	43.3	1.3	49.7	2.3
	G_NIST612_5	41.98	0.52	104250	970	11224	94	70.8	3.5	85270	860	43.9	1.5	52	2.2
Fibrous Quartz 1	Vein_Quartz_1	bd	0.02	3.4	3.1	17.3	2.8	5.6	1.1	86	51	2.36	0.55	3.8	1.8
	Vein_Quartz_2	0.465	0.091	9.3	1.9	35.9	8	9.4	1.6	35	26	1.98	0.5	bd	0.82
	Vein_Quartz_3	bd	0.016	23.3	3.8	17.1	1	14	3.2	42	32	1.75	0.47	bd	0.9
	Vein_Quartz_4	bd	0.028	6.3	1.5	13.3	1.8	5.8	1.4	42	31	1.52	0.43	bd	1.3
	Vein_Quartz_5	1.48	0.24	14160	560	18100	400	105.5	4.4	77	30	1.47	0.34	14.3	6.6
	Vein_Quartz_6	0.16	0.055	7.6	2.2	17.9	4.7	1.8	1.2	16	37	2.01	0.37	bd	1.3
	Vein_Quartz_7	0.72	0.16	2.8	1.4	14.4	1.1	bd	2	32	67	1.45	0.47	bd	1.5
	Vein_Quartz_8	0.492	0.071	13.2	1.6	23.5	8	8	10	49	32	1.83	0.4	bd	1.4
Fibrous Quartz 2	Vein_Quartz_9	0.07	0.044	17.1	3.3	25.1	1.7	5	1.2	2	43	1.88	0.61	bd	1.5
	Vein_Quartz_10	0.584	0.074	9.8	1.2	20.34	0.8	4.19	0.95	27	32	1.53	0.41	2	1.5
	Vein_Quartz_11	0.046	0.029	9.2	2.5	11.7	1.8	4.7	1.6	32	50	1.84	0.52	3.3	3.1
	Vein_Quartz_12	0.24	0.08	7.3	1.8	21.48	0.69	3.8	1.3	9	33	1.37	0.43	bd	1.5
	Vein_Quartz_13	bd	0.02	8.6	1.2	14.63	0.64	3.41	0.76	bd	26	1.02	0.3	9.1	2.4
	Vein_Quartz_14	0.581	0.076	28.4	2.7	28.8	1.4	6.27	0.97	bd	26	1.03	0.36	1.9	1.1
	Vein_Quartz_15	1.87	0.41	17.7	2.3	55	11	7	1.5	bd	20	1.2	0.3	bd	1.1
	Vein_Quartz_16	0.142	0.068	5.5	2.2	12.8	2.2	2.1	1.1	bd	29	1.55	0.5	3.6	3.2
	Vein_Quartz_17	0.273	0.067	12.5	2.4	20.3	0.87	2.91	0.97	5	29	1.27	0.31	43	59
	Vein_Quartz_18	bd	0.02	14.6	1.4	24.74	0.83	4.86	0.68	66	37	1.28	0.32	17.1	2.5
	Vein_Quartz_19	0.067	0.028	10.3	2.1	15.65	0.82	2.5	1.4	43	24	1.22	0.34	bd	0.94
	Vein_Quartz_20	1.47	0.31	17.7	2.4	37.5	5.6	5.3	1.7	27	28	1.57	0.42	bd	0.86

	Spot Label													
Blocky Quartz	Vein_Quartz_21	0.128	0.043	6.7	1.3	11.91	0.54	bd	1.1	64	43	1.08	0.32	bd	0.91
	Vein_Quartz_22	0.189	0.056	11.2	2.9	15.7	7	bd	0.81	30	25	1.55	0.45	bd	0.94
	Vein_Quartz_23	bd	0.018	15.5	2.8	13.4	1.2	3.33	0.95	66	28	1.25	0.32	4.1	5.3
	Vein_Quartz_24	0.259	0.074	17.6	3.3	23.69	0.83	1.9	2.1	80	39	1.02	0.41	bd	1.7
	Vein_Quartz_25	bd	0.052	22.5	3.3	20.63	0.76	4	1.9	38	51	1.07	0.44	bd	1.3
	Vein_Quartz_26	0.093	0.033	28	1.6	25.1	1.2	6.1	1.2	13	29	1.15	0.37	bd	0.55
	Vein_Quartz_27	0.11	0.047	7.6	1.3	17.86	0.69	bd	1	39	37	1.48	0.35	bd	1
	Vein_Quartz_28	bd	0.012	7.2	1	9.8	1.9	2.4	4.6	31	33	1.05	0.28	20	25
	Vein_Quartz_29	bd	0.022	4.14	0.79	7.76	0.98	bd	1.5	65	38	1.25	0.33	bd	0.83
	Vein_Quartz_30	bd	0.025	5.3	1.7	10.99	0.55	bd	0.82	21	29	1.46	0.41	2.1	1.4
	Vein_Quartz_31	0.53	0.15	7.6	2	36.9	5.6	4.5	1.2	49	30	1.37	0.32	bd	0.75
	Vein_Quartz_32	bd	0.016	9.2	2.2	17.7	1.3	8.77	0.87	31	21	1.06	0.27	6.5	2
	Vein_Quartz_33	bd	0.015	bd	0.89	7.58	0.8	bd	0.99	7	29	0.83	0.29	bd	1.1
	Vein_Quartz_34	bd	0.019	29.6	3.1	11.26	0.42	5.07	0.79	36	24	1.25	0.29	bd	0.51
	Vein_Quartz_35	0.183	0.041	8.16	0.99	19.98	0.73	5.44	0.96	34	33	1.22	0.35	bd	0.74
	Vein_Quartz_36	0.049	0.019	30.8	4.6	10.89	0.5	5.7	0.97	27	17	1.24	0.24	bd	0.72
	Vein_Quartz_37	0.03	0.02	6.34	0.73	15.74	0.83	bd	0.88	37	23	1.22	0.36	bd	0.81
	Vein_Quartz_38	0.062	0.026	28.6	3.7	12.32	0.95	2.5	1	58	35	1.17	0.32	bd	0.79
	Vein_Quartz_39	0.096	0.03	17.3	1.9	11.96	0.86	3.4	1.3	37	31	1.03	0.24	bd	0.94
	Vein_Quartz_40	0.17	0.048	26.8	1.7	26.81	0.93	8.5	1.7	52	42	1.19	0.4	bd	0.95

	Spot Label	Ga69		Ge72		As75		Sr88		Sn118		Sb121		Ba137	
		(ppm)	2SE (ppm)	(ppm)	2SE (ppm)	(ppm)	2SE (ppm)	(ppm)	2SE (ppm)	(ppm)	2SE (ppm)	(ppm)	2SE (ppm)	(ppm)	2SE (ppm)
Standards	G_NIST612_1	36.1	0.35	34.55	0.68	36.5	1.6	78.5	1.1	38.2	0.77	37.42	0.56	40.03	0.82
	G_NIST612_2	35.93	0.39	35.35	0.79	36.4	1.2	77.81	0.82	38.07	0.57	38.46	0.48	39	0.75
	G_NIST612_3	35.9	0.55	35.34	0.62	38	1.2	79.03	0.91	37.47	0.65	38.14	0.58	40.05	0.79
	G_NIST612_4	35.85	0.37	35.24	0.64	38.4	1.1	78.62	0.93	38.13	0.51	38.4	0.46	40.24	0.87
	G_NIST612_5	36.16	0.38	34.54	0.66	35.89	0.97	78.06	0.97	38.07	0.6	37.5	0.47	39.35	0.84

Fibrous Quartz 1	Vein_Quartz_1	0.219	0.042	1.23	0.24	bd	0.31	0.152	0.032	1.19	0.1	0.114	0.052	0.81	0.21
	Vein_Quartz_2	0.157	0.045	1.18	0.27	bd	0.35	0.144	0.035	1.34	0.16	0.31	0.12	0.59	0.18
	Vein_Quartz_3	0.114	0.031	0.83	0.23	0.73	0.5	0.229	0.055	1.38	0.16	0.398	0.099	0.53	0.18
	Vein_Quartz_4	0.193	0.057	1.58	0.31	bd	0.44	0.079	0.032	1.37	0.11	0.175	0.079	1.95	0.54
	Vein_Quartz_5	1.359	0.08	1.19	0.22	bd	0.25	16.2	1.7	1.5	0.14	0.376	0.078	5.56	0.43
	Vein_Quartz_6	0.153	0.049	1.58	0.31	bd	0.33	0.08	0.051	1.43	0.15	0.19	0.056	0.094	0.078
	Vein_Quartz_7	bd	0.045	1.69	0.47	bd	0.72	0.02	0.016	1.22	0.24	bd	0.064	bd	1
	Vein_Quartz_8	0.104	0.041	1.42	0.23	bd	0.41	0.138	0.03	1.48	0.16	0.63	0.11	0.44	0.35
Fibrous Quartz 2	Vein_Quartz_9	0.217	0.094	0.93	0.29	bd	0.5	0.214	0.036	1.19	0.15	0.59	0.13	1.82	0.37
	Vein_Quartz_10	0.095	0.037	2.26	0.3	bd	0.36	0.053	0.018	1.34	0.12	0.363	0.088	0.325	0.087
	Vein_Quartz_11	bd	0.049	2.2	0.67	bd	0.45	0.42	0.21	1.29	0.27	0.61	0.14	0.21	0.12
	Vein_Quartz_12	0.097	0.049	2.7	0.32	bd	0.33	0.092	0.021	1.15	0.14	0.58	0.12	0.5	0.2
	Vein_Quartz_13	0.215	0.058	2.11	0.29	bd	0.34	0.099	0.032	0.91	0.14	0.206	0.062	2.05	0.31
	Vein_Quartz_14	0.27	0.056	2.13	0.23	bd	0.28	0.401	0.053	1.27	0.1	0.487	0.088	2.61	0.36
	Vein_Quartz_15	0.177	0.04	2.58	0.26	bd	0.25	0.237	0.037	1.1	0.12	1.3	0.23	1.33	0.25
	Vein_Quartz_16	0.139	0.048	1.72	0.34	bd	0.31	0.105	0.044	1.23	0.21	bd	0.059	0.77	0.3
	Vein_Quartz_17	0.174	0.043	1.92	0.29	bd	0.35	0.237	0.039	1.3	0.15	0.23	0.063	1.12	0.27
	Vein_Quartz_18	0.575	0.084	2.19	0.31	bd	0.25	0.36	0.069	1.08	0.14	0.246	0.072	5.87	0.58
	Vein_Quartz_19	0.162	0.038	2.03	0.23	bd	0.17	0.39	0.11	1.17	0.14	0.131	0.059	0.54	0.13
	Vein_Quartz_20	0.171	0.044	1.47	0.28	bd	0.29	0.382	0.06	0.88	0.13	0.324	0.071	1.18	0.23
Blocky Quartz	Vein_Quartz_21	0.093	0.035	2.13	0.23	bd	0.33	0.041	0.015	1.31	0.18	bd	0.05	0.13	0.067
	Vein_Quartz_22	0.135	0.043	1.93	0.25	bd	0.24	0.157	0.03	1.36	0.14	0.31	0.064	0.49	0.18
	Vein_Quartz_23	0.174	0.043	2.06	0.3	bd	0.25	0.228	0.093	1.36	0.12	0.366	0.067	1.01	0.22
	Vein_Quartz_24	0.206	0.056	2.2	0.37	bd	0.43	0.169	0.042	1.09	0.14	0.58	0.13	1.63	0.27
	Vein_Quartz_25	0.187	0.063	2.16	0.35	bd	0.69	0.219	0.04	1.31	0.21	2.14	0.24	1.77	0.45
	Vein_Quartz_26	0.227	0.068	1.85	0.29	bd	0.27	0.401	0.072	1.19	0.18	0.439	0.083	2.19	0.32
	Vein_Quartz_27	0.179	0.057	2.08	0.4	bd	0.33	0.115	0.032	1.15	0.13	0.205	0.071	1.63	0.32
	Vein_Quartz_28	0.115	0.032	1.39	0.18	bd	0.22	0.054	0.017	1.22	0.092	0.338	0.067	0.45	0.12

Vein_Quartz_29	0.088	0.032	2.19	0.3	bd	0.27	0.041	0.017	1.49	0.19	0.081	0.047	0.259	0.09
Vein_Quartz_30	0.128	0.047	1.7	0.26	bd	0.26	0.079	0.024	1.32	0.14	0.267	0.065	0.36	0.11
Vein_Quartz_31	0.157	0.04	2.22	0.23	bd	0.22	0.067	0.021	1.85	0.19	0.303	0.057	0.81	0.29
Vein_Quartz_32	0.17	0.039	1.78	0.18	bd	0.22	0.221	0.04	1.17	0.12	0.755	0.086	0.577	0.093
Vein_Quartz_33	0.224	0.051	2.37	0.24	bd	0.3	0.016	0.0088	1.62	0.15	bd	0.035	1.42	0.28
Vein_Quartz_34	0.129	0.033	2.41	0.25	bd	0.19	0.301	0.046	1.7	0.18	0.432	0.062	0.46	0.11
Vein_Quartz_35	0.123	0.029	1.76	0.27	bd	0.2	0.094	0.024	1.3	0.14	0.536	0.083	0.182	0.074
Vein_Quartz_36	0.112	0.034	1.47	0.18	bd	0.28	0.077	0.019	1	0.12	0.324	0.05	0.414	0.095
Vein_Quartz_37	0.163	0.036	1.36	0.28	bd	0.18	0.265	0.034	1.43	0.16	0.529	0.089	1.23	0.15
Vein_Quartz_38	0.17	0.043	1.3	0.25	bd	0.31	0.135	0.028	1.3	0.19	0.581	0.094	0.71	0.22
Vein_Quartz_39	0.2	0.054	1.86	0.24	bd	0.27	0.48	0.12	1.12	0.16	0.299	0.069	0.7	0.13
Vein_Quartz_40	0.234	0.047	1.95	0.25	1	0.3	0.724	0.071	1.29	0.18	2.55	0.2	1.11	0.19

Table 6: *Sample 'SH3_Thick'. 'bd' = below detection limits.*

	Sample Number	Li7		Na23		Al27		K39		Ca43		Ti47		Fe57	
		(ppm)	2SE (ppm)	(ppm)	2SE (ppm)	(ppm)	2SE (ppm)	(ppm)	2SE (ppm)	(ppm)	2SE (ppm)	(ppm)	2SE (ppm)	(ppm)	2SE (ppm)
Standards	G_NIST612_1	42.03	0.36	104110	570	11222	53	66.4	2.4	85110	640	43.3	1.2	52.5	2.3
	G_NIST612_2	42.08	0.42	103790	690	11097	63	65.7	3.2	84730	780	45	1.4	49.5	1.8
	G_NIST612_3	41.75	0.4	103400	740	11096	66	68.2	4.2	85060	860	44.3	1.2	51.5	1.6
	G_NIST612_4	42.21	0.46	103590	560	11205	67	65.8	2.3	85120	920	44.1	1.3	50.7	1.9
	G_NIST612_5	41.99	0.52	104670	870	11201	76	66.5	2.8	84980	900	43.4	1.5	51.4	2.2
Blocky Quartz 1	Quartz_Vein_1	0.675	0.077	bd	0.81	26	1.2	3.6	0.92	bd	32	1.51	0.36	bd	2.2
	Quartz_Vein_2	2.79	0.18	4.11	0.86	35.96	0.9	3.9	0.84	bd	30	1.96	0.38	bd	0.72
	Quartz_Vein_3	1.06	0.11	3.36	0.53	37.92	0.85	4.95	0.87	bd	26	1.92	0.44	bd	0.8
	Quartz_Vein_4	bd	0.017	bd	0.92	5.35	0.27	1.8	1.1	bd	30	1.88	0.36	bd	1.2
	Quartz_Vein_5	0.3	0.054	2.37	0.94	19.64	0.75	bd	0.99	bd	43	1.46	0.36	bd	0.95
	Quartz_Vein_6	0.146	0.092	6.9	2.7	11.06	0.8	bd	0.98	bd	28	1.5	0.34	bd	1.1
	Quartz_Vein_7	bd	0.026	bd	1.1	5.44	0.34	bd	1.3	bd	46	1.41	0.42	bd	1.3
	Quartz_Vein_8	0.058	0.022	2.86	0.78	5.84	0.37	1.44	0.86	bd	24	1.53	0.37	bd	1
	Quartz_Vein_9	5.03	0.18	2.42	0.54	36.4	1	bd	0.69	bd	21	1.82	0.27	bd	0.47
	Quartz_Vein_10	1.5	0.1	2.33	0.81	33.89	0.82	bd	0.9	bd	26	1.8	0.37	bd	0.84
Fibrous Quartz	Quartz_Vein_11	0.277	0.05	10.4	1.6	9.89	0.48	5.2	1.1	bd	20	1.51	0.34	bd	0.82
	Quartz_Vein_12	0.915	0.096	3.24	0.76	26.96	0.84	4.2	1.2	bd	26	1.7	0.35	bd	1.6
	Quartz_Vein_13	0.526	0.063	bd	0.67	6.81	0.42	bd	0.78	bd	24	1.32	0.26	bd	0.74
	Quartz_Vein_14	0.054	0.026	3.73	0.75	8.81	0.66	2.7	1.5	bd	36	1.26	0.46	bd	1.2
	Quartz_Vein_15	1.4	0.14	5.9	1.3	21.11	0.53	bd	0.86	bd	30	1.31	0.26	bd	0.74
	Quartz_Vein_16	0.297	0.066	bd	0.78	11.01	0.94	bd	0.85	bd	31	1.54	0.34	bd	0.73
	Quartz_Vein_17	0.148	0.04	8.9	2.5	32.8	4.4	10.8	2.3	bd	33	1.81	0.38	36	19
	Quartz_Vein_18	0.678	0.06	11.2	1.6	30.67	0.61	3.86	0.81	bd	22	1.39	0.31	bd	0.65
	Quartz_Vein_19	0.18	0.04	9.1	1	21.2	0.82	4.12	0.93	bd	24	1.47	0.38	9	2.8
	Quartz_Vein_20	0.729	0.084	bd	1.2	26.59	0.99	bd	0.83	bd	28	1.36	0.33	bd	1

	Sample Number	(ppm)	2SE (ppm)	(ppm)	2SE (ppm)	(ppm)	2SE (ppm)	(ppm)	2SE (ppm)	(ppm)	2SE (ppm)	(ppm)	2SE (ppm)	(ppm)	2SE (ppm)
Blocky Quartz 2	Quartz_Vein_21	1.56	0.22	bd	1.8	24.39	0.84	4.1	1.1	bd	25	1.44	0.31	bd	0.88
	Quartz_Vein_22	bd	0.014	bd	1.4	3.65	0.31	3.01	0.87	bd	32	1.59	0.41	bd	1.6
	Quartz_Vein_23	0.473	0.086	bd	1.6	8.95	0.44	2.3	1	bd	36	1.42	0.37	bd	0.89
	Quartz_Vein_24	0.398	0.059	bd	0.64	19.78	0.55	3.65	0.93	bd	23	1.5	0.31	bd	0.72
	Quartz_Vein_25	0.561	0.084	bd	0.83	16.16	0.55	2.7	1	bd	21	1.42	0.45	bd	1
	Quartz_Vein_26	0.563	0.067	bd	1.1	4.48	0.33	bd	0.89	bd	27	1.11	0.32	bd	0.91
	Quartz_Vein_27	0.191	0.044	2	1	4.35	0.21	2	1.1	bd	30	1.43	0.36	bd	0.8
	Quartz_Vein_28	1.45	0.11	4.8	1	29	1	2.53	0.88	bd	25	1.5	0.31	bd	0.7
	Quartz_Vein_29	0.62	0.13	10	2	10.72	0.57	bd	1.2	bd	41	1.61	0.49	bd	1.2
	Quartz_Vein_30	bd	0.031	bd	1.1	4.4	0.3	bd	1.1	bd	39	1.76	0.42	bd	0.97
	Quartz_Vein_31	2.18	0.42	24.9	5.1	15.6	1.5	4	1.4	bd	25	1.57	0.35	bd	0.83
	Quartz_Vein_32	2.02	0.11	bd	0.82	25.24	0.74	bd	0.54	bd	28	1.47	0.28	bd	0.62
	Quartz_Vein_33	1.6	0.17	bd	1.2	24.31	0.79	3.14	0.99	bd	38	1.34	0.38	bd	0.93
	Quartz_Vein_34	0.286	0.072	bd	0.92	7.11	0.39	2.21	0.92	bd	25	1.35	0.38	bd	0.7
	Quartz_Vein_35	0.425	0.083	9.3	1.6	6.82	0.35	bd	1.5	bd	50	1.02	0.44	bd	2.3
	Quartz_Vein_36	0.233	0.065	6.2	1.4	13.6	1.3	4.2	1.8	bd	54	0.96	0.42	bd	1.5
	Quartz_Vein_37	bd	0.028	bd	1.1	3.67	0.37	bd	0.98	bd	35	0.72	0.31	bd	2.1
	Quartz_Vein_38	0.575	0.095	6.88	0.88	14.54	0.89	bd	1.3	bd	34	1.35	0.47	bd	0.83
	Quartz_Vein_39	0.163	0.071	31.3	4.3	12.79	0.69	8.9	1.9	bd	50	0.89	0.42	bd	1.7
Border	Quartz_Vein_40	0.091	0.048	9.6	2.2	3.86	0.3	bd	1.3	bd	34	0.67	0.36	bd	0.96
	Quartz_Vein_41	0.064	0.025	bd	1.1	7.74	0.34	bd	1.5	bd	36	1.86	0.59	bd	0.88

	Sample Number	Ga69		Ge72		As75		Sr88		Sn118		Sb121		Ba137	
		(ppm)	2SE (ppm)	(ppm)	2SE (ppm)	(ppm)	2SE (ppm)	(ppm)	2SE (ppm)	(ppm)	2SE (ppm)	(ppm)	2SE (ppm)	(ppm)	2SE (ppm)
Standards	G_NIST612_1	35.89	0.41	34.84	0.47	35.7	1.2	78.14	0.64	37.96	0.4	37.5	0.51	39.45	0.87
	G_NIST612_2	36.02	0.31	35.03	0.6	38	1.2	78.42	0.76	38.03	0.47	38.52	0.6	39.83	0.76
	G_NIST612_3	36.16	0.38	35.64	0.6	37.89	0.94	79.25	0.72	38.08	0.51	38.65	0.48	39.79	0.82
	G_NIST612_4	35.96	0.35	34.64	0.67	37.49	0.9	78.01	0.66	38.01	0.52	37.74	0.46	39.91	0.72
	G_NIST612_5	35.94	0.42	34.88	0.59	36.22	0.79	78.3	0.78	37.92	0.62	37.82	0.43	39.43	0.8

Group	Sample													
Blocky Quartz 1	Quartz_Vein_1	0.136	0.047	1.58	0.22	bd	0.34	0.0108	0.0078	1.179	0.097	bd	0.032	0.024	0.034
	Quartz_Vein_2	0.109	0.037	1.71	0.28	bd	0.31	0.0203	0.0087	1.71	0.18	0.214	0.056	bd	1
	Quartz_Vein_3	0.094	0.03	1.74	0.31	bd	0.35	0.001	0.0019	1.07	0.12	0.224	0.064	bd	1
	Quartz_Vein_4	0.088	0.028	1.44	0.21	1.14	0.56	0.0017	0.0024	0.98	0.17	bd	0.033	bd	1
	Quartz_Vein_5	0.1	0.045	1.63	0.23	bd	0.42	0.0024	0.0033	1.48	0.21	bd	0.043	bd	1
	Quartz_Vein_6	0.142	0.044	1.93	0.24	bd	0.4	0.096	0.042	1.32	0.16	0.16	0.063	0.92	0.17
	Quartz_Vein_7	bd	0.034	1.13	0.33	bd	0.33	bd	1	0.84	0.15	bd	0.042	0.022	0.031
	Quartz_Vein_8	0.081	0.036	1.47	0.27	bd	0.38	0.071	0.017	1.25	0.16	bd	0.025	0.089	0.045
	Quartz_Vein_9	0.059	0.025	1.92	0.23	bd	0.2	0.0005	0.0011	0.989	0.095	0.28	0.042	bd	1
	Quartz_Vein_10	bd	0.03	1.43	0.26	bd	0.3	0.0033	0.0031	1.23	0.14	0.281	0.074	bd	1
Fibrous Quartz	Quartz_Vein_11	0.127	0.034	1.4	0.21	1.48	0.46	0.179	0.03	1.16	0.12	0.122	0.046	0.366	0.096
	Quartz_Vein_12	bd	0.02	1.89	0.31	bd	0.32	0.026	0.01	1.29	0.14	0.122	0.06	0.064	0.047
	Quartz_Vein_13	0.089	0.031	1.5	0.23	bd	0.26	0.0028	0.0033	1.28	0.17	bd	0.032	bd	1
	Quartz_Vein_14	bd	0.038	1.28	0.24	bd	0.33	0.034	0.015	1.79	0.25	bd	0.059	0.025	0.027
	Quartz_Vein_15	0.089	0.03	1.83	0.29	bd	0.29	0.033	0.013	1.71	0.17	bd	0.048	0.0046	0.0091
	Quartz_Vein_16	0.095	0.03	1.44	0.19	bd	0.28	0.002	0.0022	1.56	0.17	bd	0.03	0.0031	0.0061
	Quartz_Vein_17	0.153	0.042	1.51	0.3	1.77	0.97	0.34	0.14	1.79	0.2	0.6	0.13	0.74	0.23
	Quartz_Vein_18	0.098	0.025	1.79	0.21	bd	0.23	0.053	0.015	1.39	0.14	0.162	0.052	0.317	0.088
	Quartz_Vein_19	0.076	0.028	1.74	0.24	1.6	0.63	0.12	0.029	1.79	0.15	0.191	0.056	0.222	0.073
	Quartz_Vein_20	bd	0.032	2.07	0.29	bd	0.29	0.0142	0.0083	1.67	0.17	bd	0.043	bd	1
Blocky Quartz 2	Quartz_Vein_21	0.085	0.038	1.55	0.38	bd	0.3	0.0103	0.0075	1.71	0.14	bd	0.052	bd	1
	Quartz_Vein_22	0.075	0.035	1.09	0.21	bd	0.34	bd	0.0034	1.44	0.13	bd	0.04	0.015	0.022
	Quartz_Vein_23	0.077	0.042	1.38	0.31	1.8	1.2	0.107	0.026	1.42	0.16	bd	0.056	0.066	0.05
	Quartz_Vein_24	bd	0.026	1.8	0.23	bd	0.25	0.0124	0.0076	1.82	0.18	bd	0.035	0.009	0.013
	Quartz_Vein_25	0.079	0.037	1.57	0.21	bd	0.29	bd	1	1.63	0.16	bd	0.04	bd	1
	Quartz_Vein_26	bd	0.032	1.2	0.22	bd	0.21	bd	1	1.57	0.19	bd	0.031	bd	1
	Quartz_Vein_27	bd	0.027	1.52	0.18	bd	0.3	bd	1	1.43	0.19	bd	0.048	bd	1
	Quartz_Vein_28	bd	0.035	1.45	0.26	bd	0.17	0.074	0.019	1.43	0.15	bd	0.038	0.102	0.044
	Quartz_Vein_29	bd	0.038	1.53	0.35	bd	0.34	0.021	0.015	1.49	0.23	bd	0.035	0.01	0.019

	Quartz_Vein_30	bd	0.029	1.55	0.29	bd	0.28	bd	1	1.78	0.15	bd	0.038	bd	1
	Quartz_Vein_31	bd	0.032	1.94	0.23	1.27	0.32	0.06	0.023	1.46	0.13	bd	0.033	0.11	0.051
	Quartz_Vein_32	bd	0.019	1.97	0.24	0.44	0.2	0.0058	0.0042	1.47	0.12	bd	0.031	bd	1
	Quartz_Vein_33	bd	0.031	1.75	0.32	bd	0.31	0.0087	0.0068	1.54	0.15	0.114	0.051	bd	1
	Quartz_Vein_34	0.08	0.033	1.37	0.28	bd	0.3	0.0009	0.0018	1.53	0.14	bd	0.035	0.009	0.013
	Quartz_Vein_35	0.097	0.045	1.31	0.29	bd	0.46	0.0057	0.0088	1.63	0.22	0.163	0.057	bd	1
	Quartz_Vein_36	0.135	0.075	1.27	0.35	bd	0.27	0.0066	0.0095	1.57	0.22	bd	0.053	0.053	0.048
	Quartz_Vein_37	0.064	0.04	1.56	0.26	bd	0.43	bd	1	1.61	0.21	bd	0.051	bd	1
	Quartz_Vein_38	0.091	0.032	1.3	0.25	bd	0.3	0.134	0.031	1.51	0.19	bd	0.053	0.012	0.017
Border	Quartz_Vein_39	0.129	0.039	0.84	0.27	1.01	0.39	0.295	0.056	1.87	0.2	0.293	0.081	0.57	0.21
	Quartz_Vein_40	bd	0.04	1.31	0.31	bd	0.37	0.019	0.014	2	0.2	bd	0.045	0.01	0.019
	Quartz_Vein_41	bd	0.032	1.41	0.28	bd	0.25	0.002	0.0028	1.77	0.18	bd	0.051	0.007	0.015